Alcohol 107 (2023) 56–72

Contents lists available at ScienceDirect

Alcohol

journal homepage: http://www.alcoholjournal.org/

Precocious emergence of cognitive and synaptic dysfunction in 3xTg-AD mice exposed prenatally to ethanol

Adelaide R. Tousley [a, b], Pamela W.L. Yeh [a], Hermes H. Yeh [a, *]

[a] Department of Molecular and Systems Biology, Geisel School of Medicine at Dartmouth, Hanover, NH, United States
[b] MD-PhD Program, Geisel School of Medicine at Dartmouth; Integrative Neuroscience at Dartmouth Graduate Program, Hanover, NH, United States

ARTICLE INFO

Article history:
Received 17 May 2022
Received in revised form
1 August 2022
Accepted 9 August 2022

Keywords:
Alzheimer's disease
FASD
GABAergic interneuron
Gestational ethanol
Learning/memory
Synaptic transmission

ABSTRACT

Alzheimer's disease (AD) is the most common cause of dementia, affecting approximately 50 million people worldwide. Early life risk factors for AD, including prenatal exposures, remain underexplored. Exposure of the fetus to alcohol (ethanol) is not uncommon during pregnancy, and may result in physical, behavioral, and cognitive changes that are first detected during childhood but result in lifelong challenges. Whether or not prenatal ethanol exposure may contribute to Alzheimer's disease risk is not yet known. Here we exposed a mouse model of Alzheimer's disease (3xTg-AD), bearing three dementia-associated transgenes, presenilin1 (PS1M146V), human amyloid precursor protein (APPSwe), and human tau (TauP301S), to ethanol on gestational days 13.5–16.5 using an established binge-type maternal ethanol exposure paradigm. We sought to investigate whether prenatal ethanol exposure resulted in a precocious onset or increased severity of AD progression, or both. We found that a brief binge-type gestational exposure to ethanol during a period of peak neuronal migration to the developing cortex resulted in an earlier onset of spatial memory deficits and behavioral inflexibility in the progeny, as assessed by performance on the modified Barnes maze task. The observed cognitive changes coincided with alterations to both GABAergic and glutamatergic synaptic transmission in layer V/VI neurons, diminished GABAergic interneurons, and increased β-amyloid accumulation in the medial prefrontal cortex. These findings provide the first preclinical evidence for prenatal ethanol exposure as a potential factor for modifying the onset of AD-like behavioral dysfunction and set the groundwork for more comprehensive investigations into the underpinnings of AD-like cognitive changes in individuals with fetal alcohol spectrum disorders.

Introduction

Alzheimer's disease (AD) is a progressive neurodegenerative condition characterized clinically by cognitive impairment, including memory and language deficits, and pathologically by synaptic loss, tau neurofibrillary tangles, amyloid β plaques, and glial activation (Hardy & Selkoe, 2002; Knopman et al., 2021; Naseri, Wang, Guo, Sharma, & Luo, 2019). Alzheimer's disease is the most common cause of dementia, currently affecting an estimated 50 million people worldwide, and cases are expected to triple by 2050 (Patterson, 2018). Both genetic and environmental factors have been reported to increase the risk for developing AD, though studies of environmental risk factors have largely focused on lifestyle choices and comorbidities in adulthood (Edwards, Gamez, Escobedo, Calderon, & Moreno-Gonzalez, 2019; Pimenova, Raj, & Goate, 2018). In this light, early risk factors for AD remain largely underexplored (Seifan, Schelke, Obeng-Aduasare, & Isaacson, 2015; Yu et al., 2020). Identifying early risk factors for AD may contribute to extending the period for modifying disease progression. In the least, it will increase the time that affected individuals and their potential caregivers have to plan for the future (Rasmussen & Langerman, 2019).

Prenatal exposure to ethanol is common: One in 9 pregnant women in the United States report having consumed ethanol in the last 30 days and, of those, approximately one-third report binge drinking (Denny, 2019). This exposure can result in considerable physical, cognitive, and behavioral impairments in the progeny that persist into adulthood (Wozniak, Riley, & Charness, 2019).

* Corresponding author. Department of Molecular and Systems Biology, Geisel School of Medicine at Dartmouth, 66 College Street, Hanover, NH 03755, United States. Tel.: +1 603 381 2059.
E-mail address: Hermes.Hsiao-mei.Yeh@dartmouth.edu (H.H. Yeh).

https://doi.org/10.1016/j.alcohol.2022.08.003

Outcomes following a prenatal exposure to ethanol depend upon factors such as drinking pattern, dose, and timing of ethanol exposure, all of which can contribute to developing fetal alcohol spectrum disorder (FASD) (Jacobson et al., 2021; May & Gossage, 2011; Wozniak et al., 2019). Individuals with FASD experience challenges in learning, memory, language skills, and comprehension, which contribute to difficulties in academic performance, as well as social and professional challenges across their lifespans (Davis, Gagnier, Moore, & Todorow, 2013; Mattson, Crocker, & Nguyen, 2011; Rasmussen, 2005).

Alcohol exposure during adulthood is a risk factor for AD pathology in humans (Heymann et al., 2016; Huang, Zhang, & Chen, 2016; Koch et al., 2020; Peng et al., 2020). Remarkably, many cognitive impairments identified in FASD individuals are reminiscent of those identified as early-life risk factors for AD. Indeed, there is a growing appreciation that prenatal ethanol exposure may also increase risk for developing adult-onset diseases, including heart disease, type II diabetes, autoimmune diseases, and certain cancers (Lunde et al., 2016; Moore & Riley, 2015). However, whether prenatal ethanol exposure may influence any aspect of AD pathogenesis during aging is not yet known. In this study, we asked whether and how prenatal exposure to ethanol might be a risk factor for contributing to the development or progression, or both, of AD.

We examined the effects of a brief ethanol exposure *in utero* on spatial learning/memory, behavioral flexibility, synaptic function, interneuron number, and the disposition of β-amyloid histopathology in a transgenic mouse model of AD (3xTg-AD). We have previously shown that an exposure to ethanol during embryonic days (E) 13.5–16.5 results in altered neuronal migration, synaptic activity, and behavior in neonatal, adolescent, and young adult mice (Delatour, Yeh, & Yeh, 2019a, 2019b; Skorput, Gupta, Yeh, & Yeh, 2015; Skorput, Lee, Yeh, & Yeh, 2019). Here we applied the same prenatal ethanol exposure paradigm to pregnant 3xTg-AD mice, which harbor three dementia-associated transgenes encoding presenilin1 ($PS1_{M146V}$), human amyloid precursor protein (APP_{Swe}), and human tau (Tau_{P301S}), under the Thy1 promoter (Campsall, Mazerolle, De Repentingy, Kothary, & Wallace, 2002; Oddo et al., 2003). In contrast to other mouse models of AD, 3xTg-AD mice develop A-b and tau pathology concurrently with the onset of spatial memory deficits by 6 months of age (Billings, Oddo, Green, McGaugh, & LaFerla, 2005; Mastrangelo & Bowers, 2008; Oddo et al., 2003). Notably, ethanol exposure has been reported to modify both the AD neuropathology and behavior of adult 3xTg-AD mice (Barnett et al., 2022; Hoffman et al., 2019; Muñoz et al., 2015). Based on findings in this study, we report that a brief prenatal exposure to ethanol during a period of peak neuronal migration in the embryonic cortex (embryonic day [E] 13.5–16.5) results in a precocious emergence of spatial memory deficits and behavioral inflexibility in 4-month-old 3xTg-AD mice, but does not exacerbate their severity in 6-month-old 3xTg-AD mice. In addition, this precocious onset of behavioral abnormality is associated with changes in synaptic connectivity and number of parvalbumin-expressing (PV+) GABAergic interneurons, and degree of β-amyloid deposition in the medial prefrontal cortex (mPFC). Thus, our findings suggest that prenatal alcohol exposure may modify the susceptibility of 3xTg-AD mice to the pathological progression of AD.

Methods

Transgenic mice

B6129SF1/J (B6129) (Jackson Labs #101045) and B6;129-Tg(APPSwe,tauP301L)1Lfa *Psen1*^{tm1Mpm}/Mmjax (3xTg-AD) mice (MMRC# 034830-JAX) were bred and maintained following the guidelines and procedures prescribed by NIH *Guide for Animal Care and Use*, and approved by Dartmouth College's Institutional Care and Use Committee. Animals were housed on a 12-h light/dark cycle with light periods occurring between 7:00 AM and 7:00 PM.

Ethanol exposure paradigm and experimental timeline

In line with a previously described binge-type ethanol exposure paradigm (Delatour et al., 2019a, 2019b; Skorput et al., 2015, 2019), single pairs of male and female mice were housed overnight for breeding with the following day designated as embryonic day (E) 0.5 (Fig. 1A).

Pregnant dams were allowed access *ad libitum* to either 5% (w/w) ethanol in liquid diet or lab chow (5V5M, ScottPharma Solutions) from E13.5 to E16.5. We have previously compared control groups fed *ad libitum* with those pair-fed an isocaloric maltose liquid diet and detected no significant differences (Cuzon, Yeh, Yanagawa, Obata, & Yeh, 2008). Thus, for the sake of efficiency, the pair-fed diet control group was excluded. Dams were weighed and liquid diet was replaced daily, with water available *ad libitum*. E13.5 to 16.5 is a critical gestational time span for the peak of migration of primordial GABAergic interneurons and pyramidal neurons into the cortical plate of the embryonic cortex (Batista-Brito & Fishell, 2009; Clancy, Darlington, & Finlay, 2001).

3xTg-AD dams drank to a mean blood ethanol concentration (BEC) of 49.17 mg/dL ± 14.03 mg/dL, as measured at 11:00 PM on E15.5 using an Analox AM1 series III analyzer (Analox Instruments) (Fig. 1B). Our previous assessment of transgenic mice on congenic C57BL6J background using the same drinking paradigm resulted in binge levels of ~80 mg/dL (Skorput et al., 2015). Background strain dramatically affects ethanol preference, sensitivity, and metabolism (Bachmanov, Tordoff, & Beauchamp, 1996; Downing, Balderrama-Durbin, Broncucia, Gilliam, & Johnson, 2009; Lim, Zou, Janak, & Messing, 2012). In contrast to C57BL6J mice, 129/J mice tend to have lower alcohol preference and are less susceptible to the teratogenic effects of prenatal ethanol exposure, suggesting potential differences in ethanol metabolism or genetic disposition. Hybrid B6129 mice also show decreased ethanol preference relative to C57BL6J mice (Bachmanov et al., 1996; Downing et al., 2009; Lim et al., 2012). Differences in ethanol preference, sensitivity or metabolism could also account for the decreased BEC measured in 3xTg-AD dams, given their hybrid B6129 background, relative to that attained by congenic C57BL6J transgenic mice.

After birth, mice were maintained to 4 months or 6 months of age, then subjected to the 10-day Barnes maze behavioral testing paradigm (see below). Following the 2-week behavioral testing, the mice were sacrificed for electrophysiology and immunohistochemistry experiments at ~4.5 and ~6.5 months, respectively (Fig. 1A). Each animal was used for behavioral testing at a single time point: 4 months or 6 months. Body weight did not differ between B6129 control or 3xTg-AD or 3xTg-AD + EtOH experimental cohorts at either 4-month or 6-month time points (two-way ANOVA, $F_{(2,50)} = 0.5151, 0.6006$) (Fig. 1C).

Modified Barnes maze testing

Barnes maze testing was conducted as described by Skorput et al. (2015, 2019), based on a modified Barnes maze protocol (Koopmans, Blokland, van Nieuwenhuijzen, & Prickaerts, 2003). The Barnes maze consists of 12 holes equally spaced around a circumferential circular wall (diameter = 95 cm), with spatial cues (large red letters) between each hole. Briefly, mice were single-housed for 3–7 days prior to initiation of the 10-day behavioral testing paradigm. Mice underwent 4 days of training during which they learned to associate escape from the maze through one of the

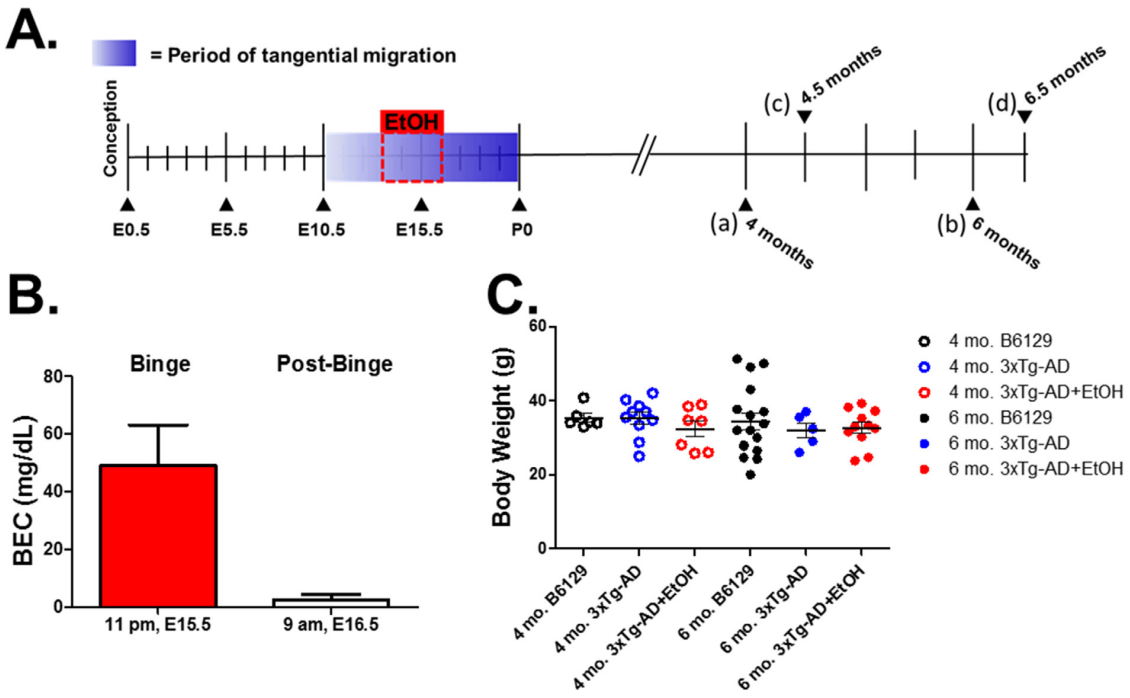

Fig. 1. Experimental timeline, blood ethanol concentration (BEC) in 3xTg-AD pregnant dams, and group-dependent differences in body weight. (**A**) Pregnant 3xTg-AD dams were exposed to ethanol during a period of peak tangential migration of GABAergic interneurons from the medial ganglionic eminence into the developing cortex: embryonic day (E) 13.5–E16.5. Mice were then aged to (a) 4 months or (b) 6 months, at which point they completed the 10-day modified Barnes maze testing paradigm. Subsequently, mice were sacrificed in the 2 weeks following behavioral testing for immunohistochemistry and/or electrophysiology experiments at (c) 4.5 months or (d) 6.5 months. (**B**) Pregnant 3xTg-AD dams drank liquid food containing ethanol (5% w/w) and yielded a mean BEC of 49.17 mg/dL at 11:00 PM on E15.5 ($N = 3$ dams) when allowed on E13.5–E16.5, while BECs had dropped to a mean of 2.66 mg/dL at 9:00 AM on E16.5 ($N = 2$ dams) (**C**) Body weight did not differ significantly in 4-month-old mice: B6129 (empty black dots, $N = 6$, $n = 6$ M, 3 litters); 3xTg-AD (empty blue dots, $N = 11$, $n = 4$ F, 7 M, 3 litters); 3xTg-AD + EtOH (empty red dots, $N = 7$, $n = 4$ F, 3 M, 2 litters); 6-month-old: B6129 (filled black dots, $N = 17$, $n = 9$ F, 8 M, 5 litters); 3xTg-AD (filled blue dots, $N = 6$, $n = 2$ F, 4 M, 4 litters); 3xTg-AD + EtOH (filled red dots $N = 12$, $n = 3$ F, 9 M, 5 litters). N = total number of mice per group, n = total number of mice by sex: F (female), M (male).

12 holes, referred to as the "escape hole", while all other holes were plugged. This acquisition phase was followed by 2 days of rest, then 2 days of testing for memory of the original escape hole, followed by 2 days of testing for reversal learning. In reversal learning, the escape hole was reversed to the quadrant of the maze opposite from the original escape hole (Fig. 2B). Memory of the escape hole was reinforced by the anxiolytic effects of returning mice to their home cage following completion of each trial. Escape holes were assigned randomly to each individual mouse and changed between mice completing testing during the same time period. Escape latency and number of errors (nose pokes in a non-escape hole) were recorded by blinded observers over 4 trials per mouse per day, lasting until a mouse poked its nose into the escape hole or a maximum of 4 min. An overhead video camera driven by video tracking software (Videomex-one, Colburn Instruments) was used to determine total distance traveled during each trial. At the beginning of each trial, the mouse was placed at the center of the modified Barnes maze and covered, with the cover removed at the initiation of a given trial. Between trials, the maze was cleaned with Clidox (Pharmacal Research). Testing was completed daily between 9:00 AM and 12:00 PM at the beginning of the light period.

Electrophysiology

Behaviorally tested mice were anesthetized with 4% isoflurane and euthanized by decapitation. The cerebral cortex was hemisected, with the left half used for electrophysiology experiments and the right half immerse fixed in 4% paraformaldehyde (PFA)/0.1 M phosphate-buffered saline (PBS) for immunohistochemistry experiments. The left hemisphere was cut to 250-μm sections with a Leica vibratome in oxygenated (95% O_2, 5% CO_2) ice-cold cutting solution ([in mM] 3 KCl, 7 $MgCl_2$, 0.5 $CaCl_2$, 1.25 NaH_2PO_4, 28 $NaHCO_3$, 8.3 D-glucose, 110 sucrose, pH 7.4 [adjusted with 1 N NaOH]), followed by at least a 1-h incubation at room temperature in oxygenated artificial cerebrospinal fluid (aCSF) ([in mM] 124 NaCl, 5.0 KCl, 2.0 $MgCl_2$, 2.0 $CaCl_2$, 1.25 NaH_2PO_4, 26 $NaHCO_3$, 10 D-glucose, pH 7.4 [adjusted with 1 N NaOH]) prior to electrophysiological recording.

Acute brain slices containing mPFC were placed in a custom-made acrylic recording chamber maintained at 32 °C and continuously perfused (0.5–1.0 mL/min) with oxygenated aCSF. Slices were visualized using a fixed-stage upright fluorescence microscope (Olympus BX51W1) with Hoffman Modulation Contrast optics. Whole-cell recordings were conducted using a MultiClamp 700B amplifier (Axon Instruments), and borosilicate glass (Sutter Instrument; OD: 1.5 mm; ID: 0.86 mm) recording electrodes were pulled with a Flaming Brown Micropipette Puller (Sutter Instrument Model P80 PC). The resistance of the recording pipettes ranged between 7 and 10 MΩ as measured in bath aCSF.

A cesium methanesulfonate-based internal solution ([in mM] 130 Cs-methanesulfonate, 10 HEPES, 0.5 EGTA, 8 NaCl, 10 Na-phosphocreatine, 1 QX-314, 4 Mg_2+ ATP, and 0.4 Na + GTP adjusted to pH 7.3 with 1 N CsOH) was used for whole-cell recording of spontaneous excitatory (sEPSC) and inhibitory (sIPSC) postsynaptic currents from Layer V/VI pyramidal neurons in the mPFC. sEPSCs and sIPSCs were isolated at holding potentials

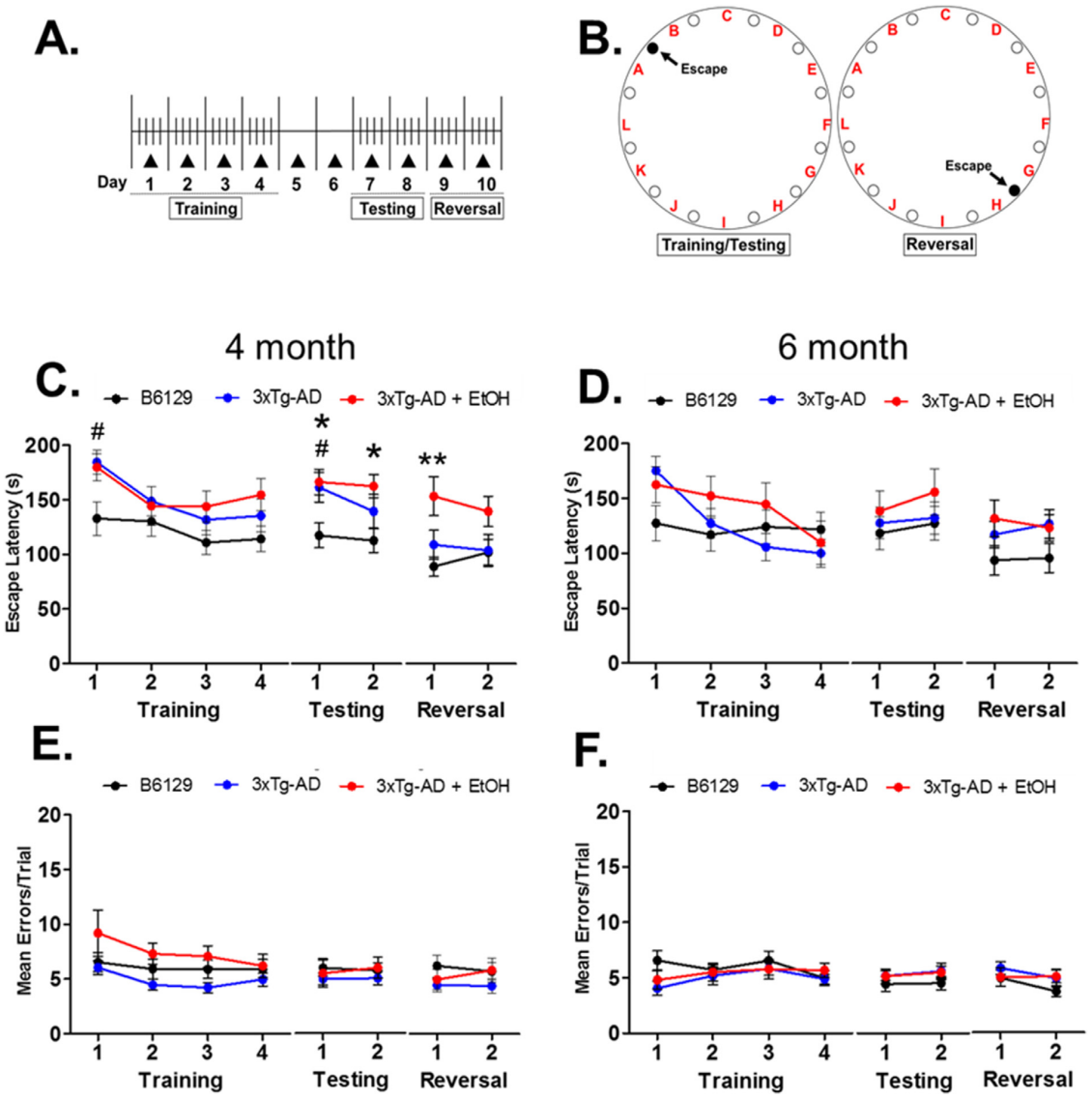

Fig. 2. Prenatal ethanol exposure results in an earlier onset of spatial memory deficits in 3xTg-AD mice, as well as deficits in reversal learning. (**A**, **B**) 4-month-old and 6-month-old mice completed the 10-day modified Barnes maze testing paradigm, consisting of a 4-day training phase, 2-day testing phase, and 2-day reversal phase (**C**, **D**) Mean latency to correctly identify the escape hole (sec, $n = 4$ trials) for B6129 (black dots connected by black lines), 3xTg-AD (blue dots connected by blue lines), and ethanol-exposed 3xTg-AD mice (red dots connected by red lines) in 4-month-old (**C**) and 6-month-old mice (**D**). (**E**, **F**) Mean errors per trial (nose pokes not in the escape hole) for B6129 (black dots connected by black lines), 3xTg-AD (blue dots connected by blue lines), and ethanol-exposed 3xTg-AD mice (red dots connected by red lines) in 4-month-old (**E**) and 6-month-old mice (**F**). (**C**) * = $p < 0.05$ B6129 vs. 3xTg-AD + EtOH, ** = $p < 0.01$ B6129 vs. 3xTg-AD + EtOH, # = $p < 0.05$ B6129 vs. 3xTg-AD, two-way repeated-measures ANOVA with Bonferroni *post hoc* tests. For sample sizes by experimental group see Table 1.

of −70 mV and 0 mV, respectively. Recordings were filtered with a 10-kHz low pass filter (Clampex Version 9.2) and digitized at 25 kHz (Digidata 1320A; Molecular Devices). Holding potential was corrected for junction potential.

Average frequency, amplitude, and charge from 2-min epochs after a 2-min baseline stabilization period at each holding potential were determined using MiniAnalysis Software (Version 6.0, Synaptosoft). Pyramidal neurons were identified in acute live brain slices by the relatively large size and laminar location of their soma. Each electrophysiologically recorded cell was also filled with recording solution containing 2% neurobiotin (Vector Laboratories) during recording (Fig. 3A, right panel). The slices containing neurobiotin-filled neurons were fixed after processing as described previously (Delatour et al., 2019b). Briefly, acute slices were fixed overnight in 4% PFA/0.1 M PBS, cryopreserved overnight in 30% sucrose/0.1 M PBS, permeabilized with 30% H_2O_2/0.1 M PBS, blocked in 10% normal goat serum (NGS)/0.4% Triton X 100, and incubated overnight at 4 °C in 10 μg/mL Streptavidin DyLight 594 (Vector Labs).

Immunohistochemistry, imaging, and image analysis

Following immersion fixation overnight in 4% PFA/0.1 M PBS, the right hemispheres were cryopreserved overnight first in 15%

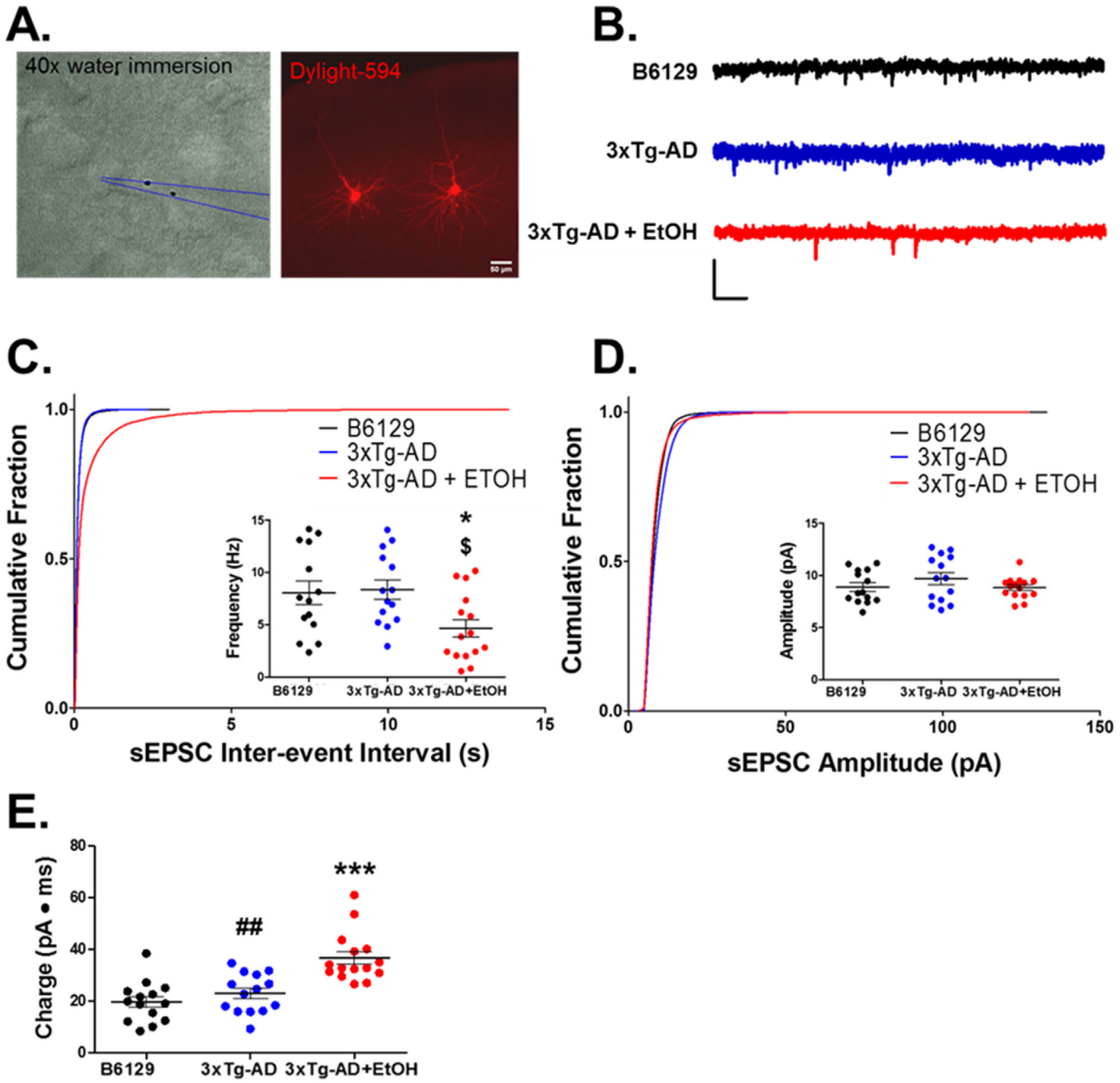

Fig. 3. Prenatal ethanol exposure decreases the frequency and increases the charge of spontaneous excitatory post-synaptic currents (sEPSCs) in the medial prefrontal cortex (mPFC) of 4-month-old 3xTg-AD mice. (**A**, left panel) 40× magnification Hoffman Modulated Contrast image of a Layer V/VI pyramidal neuron in the mPFC from a 4-month-old mouse during recording. (**A**, right panel) Image of a neurobiotin-filled pyramidal neuron after recording; scale bar = 50 μM. (**B**) Representative traces recorded under whole-cell voltage clamp of sEPSCs recorded at a holding potential −70 mV from Layer V/VI pyramidal neurons in acute mPFC slices from 4-month-old: B6129 (black), 3xTg-AD (blue), and 3xTg-AD + EtOH (red) mice; scale bar = 250 ms × 20 pA. (**C**) Cumulative distribution of sEPSC inter-event intervals (s) recorded from Layer V/VI pyramidal neurons of 4-month-old: B6129 (black), 3xTg-AD (blue), and 3xTg-AD + EtOH (red). (inset): Mean sEPSC frequency of Layer V/VI pyramidal neurons of mPFC of 4-month-old: B6129 (black dots), 3xTg-AD (blue dots), and 3xTg-AD + EtOH (red dots) mice. (**D**) Cumulative distribution of sEPSC amplitude intervals (s) recorded in Layer V/VI pyramidal neurons of 4-month-old: B6129 (black), 3xTg-AD (blue), and 3xTg-AD + EtOH (red). (inset): Mean sEPSC amplitude of Layer V/VI pyramidal neurons of mPFC of 4-month-old: B6129 (black dots), 3xTg-AD (blue dots), and 3xTg-AD + EtOH (red dots) mice. (**E**) Mean sEPSC amplitude of Layer V/VI pyramidal neurons of mPFC of 4-month-old: B6129 (black dots), 3xTg-AD (blue dots), and 3xTg-AD + EtOH (red dots) mice. (**C**) * = $p < 0.05$, B6129 vs. 3xTg-AD + EtOH, $ = $p < 0.05$ 3xTg-AD vs. 3xTg-AD + EtOH, one-way ANOVA with Bonferroni *post hoc* tests (**E**) *** = $p < 0.001$, B6129 vs. 3xTg-AD + EtOH, # = $p < 0.05$, one-way ANOVA with Bonferroni *post hoc* tests. For all measures: B6129 ($N = 14$ cells, $n = 4$ F, 5 M, 6 litters); 3xTg-AD ($N = 15$ cells, $n = 5$ F, 5 M, 6 litters); 3xTg-AD + ETOH ($N = 15$ cells, $n = 3$ F, 7 M, 7 litters). N = total number of cells per group (dots) from n = total number mice by sex: F (female), M (male).

sucrose/0.1 M PBS, then 30% sucrose/0.1 M PBS. Thirty-micron sections were obtained using a sliding microtome and collected into 0.1 M PBS. Sections were permeabilized for 30 min by incubating in 0.25% Triton X-100/10% NGS solution then overnight at 4 °C in primary antibody: rabbit anti-parvalbumin (Abcam, ab11427, 1:1000) in 0.1 M PBS, or mouse anti-β amyloid (Aβ), amino acid residue 11–16/amyloid precursor protein (APP) (6E10, BioLegend #803001, 1:200) in 0.25% Triton X-100/10% NGS. The following day, sections underwent two 30-min washes in 1X PBS, followed by overnight incubation in secondary antibody: goat anti-rabbit Alexa Fluor-488 or goat anti-mouse Alexa Fluor-555 (Invitrogen, 1:1000) in 0.1 M PBS at 4 °C. Prior to mounting, sections were washed overnight in PBS and counterstained with DAPI (Roche, 10236276001). Sections were coverslipped with FluorSave reagent (Millipore, 345789).

Images were captured by a CCD camera (Hamamatsu) using a 10 × 0.3 NA objective (Olympus) fit to a spinning disk confocal microscope (BX61WI, Olympus) and digitized using cellSens

software (Olympus). Images were then montaged using Photoshop CS2 software for a complete view of the mPFC, and cells were counted using FIJI ImageJ Cell Counter analysis plug-ins by researchers blinded to experimental group (Schindelin et al., 2012). Cells were counted in 10 equivalent serial sections from the mPFC defined rostrally by the slice where all five cortical layers of the mPFC were first observable and caudally by the presence of the corpus callosum. Relative APP/Aβ fluorescence intensity in the mPFC was assessed again from 10 serial sections from the mPFC, using FIJI ImageJ software. Calculations of relative fluorescence intensity were made as follows: relative fluorescence intensity = (APP/Aβ fluorescence intensity − Baseline fluorescence intensity)/Baseline fluorescence intensity, where fluorescence intensity = raw integrated density/area or region of interest (μm^2). Baseline fluorescence intensity measurements were made per slice for 10 equivalent serial sections.

Data analysis and statistics

Data derived from both male and female mice were pooled, and analyses were performed by experimenters blinded to genotype, exposure, and age of mice. Multifactor ANOVAs were performed using IBM SPSS statistics (version 28.0.1.0), followed by one- or two-way ANOVAs with Bonferroni *post hoc* tests where Bartlett's test for equal variances indicated data experimental groups had equal variances, and Kolmogorov–Smirnov tests demonstrated that data were normally distributed, while Kruskall–Wallis tests with Dunn's multiple comparisons *post hoc* tests were used when unequal variances were identified using GraphPad Prism (version 5.03). Repeated-measure ANOVAs were used to compare the performance (escape latency, errors, and total distance traveled) of individual mice over the course of the 4-day training, 2-day testing, and 2-day reversal periods. For behavioral experiments and counts of parvalbumin-immunoreactive cells, comparisons were made between mice from at least three litters. For electrophysiology experiments, comparisons were made between neurons from mice from at least three litters, with no more than three neurons per mouse. $p < 0.05$ was considered significant and group means presented as mean ± standard error of the mean for all analyses.

Results

Prenatal ethanol exposure results in precocious onset of spatial memory deficits and alters reversal learning in 3xTg-AD mice without exacerbating AD-like behavioral symptoms

The modified Barnes maze is a behavioral task that assesses spatial learning, memory, and behavioral flexibility over the course of three testing phases: training, testing, and reversal (Fowler et al., 2013; Koopmans et al., 2003; Vetreno & Crews, 2012). During the preliminary 4-day training phase, mice are asked to use spatial cues to identify one of the 12 holes within the Barnes maze setup as an "escape hole" (Fig. 2A and B). Following a 2-day break from exposure to the maze, memory of the original escape hole is assessed during the 2-day testing period. Mice are then asked during the reversal phase to learn to identify a novel escape hole in the maze placed on the opposite side of the original escape hole. Previous work using the same 3-day ethanol exposure paradigm uncovered a deficit in reversal learning in young adult (~2-month-old) mice in the modified Barnes maze task (Skorput et al., 2015, 2019). Here, we tested 4- and 6-month-old B6129 (control), 3xTg-AD, and 3xTg-AD + EtOH (experimental) cohorts to assess age- and ethanol exposure-dependent persistent deficits in spatial learning and memory, and behavioral flexibility (Table 1; Fig. 2C–F).

At 4 months of age, neither the control (B6129) nor the experimental groups (3xTg-AD or 3xTg-AD + EtOH) displayed altered escape latencies, total distance traveled (cm), or number of incorrect nose pokes (mean errors/trial) during the 4-day training (acquisition) phase of the modified Barnes maze paradigm (two-way repeated-measures ANOVA, escape latency: $F_{(2,147)} = 2.630$, $p = 0.0822$; total distance traveled: $F_{(2,147)} = 2.064$, $p = 0.1379$; errors: $F_{(2,147)} = 3.067$, $p = 0.0556$) (Fig. 2C, E; Supplementary Fig. 1A). Although the B6129 mice escaped the Barnes maze more quickly than 3xTg-AD mice on Training Day 1 (B6129: 132.9 ± 15.39 s; 3xTg-AD: 184.6 ± 11.3 s, $t = 2.806$, $p < 0.05$) and trended toward an improved initial performance vs. 3xTg-AD + EtOH mice (179.9 ± 12.58 s), these data suggested that, regardless of control or experimental groups, 4-month-old mice do not differ significantly in their overall ability to learn to perform the Barnes maze task.

Figure 2C illustrates that group-dependent differences in escape latency became evident in 4-month-old mice during both testing and reversal phases (two-way repeated-measures ANOVA, testing: $F_{(2,49)} = 4.881$, $p = 0.0117$; reversal: $F_{(2,49)} = 4.397$, $p = 0.0175$). Bonferroni *post hoc* tests revealed that, while B6129 and 3xTg-AD mice differed on Testing Day 1 alone (B6129: 117.1 ± 11.38 s; 3xTg-AD: 161.2 ± 13.52 s, $t = 2.565$, $p < 0.01$), 3xTg-AD + EtOH mice required significantly more time to escape the Barnes maze on both testing days relative to B6129 mice (Test Day 1: B6129:117.1 ± 11.38 s;, 3xTg-AD + EtOH: 165.9 ± 11.61 s, $t = 3.574$, $p < 0.05$; Test Day 2: B6129:112.3 ± 10.85 s; 3xTg-AD + EtOH: 162.1 ± 10.57 s, $t = 2.583$, $p < 0.05$) (Fig. 2C). In addition, the 3xTg-AD + EtOH cohort displayed increased escape latency relative to B6129 mice on Reversal Day 1, pointing to a deficit in reversal learning (Bonferroni *post hoc*, B6129: 88.74 ± 8.914 s; 3xTg-AD + EtOH: 152.9 ± 17.81 s, $t = 4.397$, $p < 0.01$) (Fig. 2C). This increase in escape latency was not accompanied by an overall increase in the number of errors ($F_{(2,49)} = 1.155$, $p = 0.3234$) (Fig. 2E), but coincided with a decrease in total distance traveled by 3xTg-AD + EtOH mice relative to B6129 mice on Test Day 1 (two-way repeated-measures ANOVA, testing: $F_{(2,49)} = 3.529$, $p = 0.037$; Bonferroni *post hoc*, B6129: 300.2 ± 25.72 cm; 3xTg-AD + EtOH: 218.0 ± 33.23 cm, $t = 2.621$, $p < 0.05$). No differences in total distance traveled were observed during the reversal phase ($F_{(2,49)} = 1.929$, $p = 0.1562$) (Supplementary Fig. 1A). These data suggest that, in contrast to the unexposed 3xTg-AD mice, the ethanol-exposed 3xTg-AD mice have more severe spatial memory deficits and a deficit in reversal learning at 4 months.

Consistent with the performance of 4-month-old mice, no group differences in escape latency were identified in 6-month-old mice during the training phase (two-way repeated-measures ANOVA, $F_{(2,147)} = 2.064$, $p = 0.1379$) or mean errors/trial ($F_{(2,159)} = 1.364$, $p = 0.2645$). This suggests that the ability to learn the Barnes maze task was not altered in the 6-month-old experimental groups over the 4-day acquisition phase (Fig. 2D). In addition, although they did not differ in escape latency, 6-month-old mice did demonstrate group-specific differences in total distance traveled during the training phase ($F_{(2,159)} = 13.82$, $p < 0.0001$). Bonferroni *post hoc*

Table 1
Age, genotype/exposure, and sex of behaviorally tested animals

Age	B6129		3xTg-AD		3xTg-AD + EtOH	
	F	M	F	M	F	M
4 months	10 (3)	9 (3)	10 (3)	10 (3)	7 (3)	6 (3)
6 months	9 (3)	11 (3)	10 (3)	11 (4)	5 (3)	10 (3)

n (*N*) where *n* = number of mice tested; *N* = number of litters included.

tests indicated that B6129 mice traveled significantly more than 3xTg-AD mice during Training Day 1 and 2 (Training Day 1: B6129, 550.4 ± 82.50 cm; 3xTg-AD, 240.9 ± 28.61 cm, $t = 5.726$, $p < 0.001$, $t = 2.565$, $p < 0.01$; Training Day 2: B6129, 370.2 ± 37.88 cm; 3xTg-AD, 222.6 ± 39.49 cm, $t = 2.731$, $p < 0.05$), and 3xTg-AD + EtOH mice on Training Day 1 (3xTg-AD + EtOH: 256.1 ± 36.38 cm, $t = 4.982$, $p < 0.001$) (Supplementary Fig. 1B).

In contrast to the 4-month-old mice, no significant differences were detected in escape latency between B6129, 3xTg-AD, and 3xTg-AD + EtOH mice during the testing and reversal phases, although 3xTg-AD + EtOH mice tended to display longer escape latencies during testing and reversal phases (Testing Day 1: 138.5 ± 18.54 s; Testing Day 2: 155.7 ± 21.17 s, Reversal Day 1: 131.4 ± 16.88 s; Reversal Day 2: 122.9 ± 12.04 s) relative to B6129 mice (Testing Day 1: 127.5 ± 14.29 s; Testing Day 2: 127.3 ± 15.32 s; Reversal Day 1: 93.39 ± 13.59 s; Reversal Day 2: 95.34 ± 13.24 s) and 3xTg-AD (Testing Day 1: 138.5 ± 18.54 s; Testing Day 2: 132.1 ± 14.57 s; Reversal Day 1: 116.8 ± 12.04 s; Reversal Day 2: 126.4 ± 12.04 s) mice (Testing: $F_{(2,53)} = 0.8528$, $p = 0.5619$; Reversal: $F_{(2,53)} = 2.136$, $p = 0.1282$) (Fig. 2D). No group-dependent differences in total distance traveled or number of errors were identified during the testing or reversal phases (Errors: Testing: $F_{(2,53)} = 0.8881$, $p = 0.4175$; Reversal: $F_{(2,53)} = 1.069$, $p = 0.3505$; Total distance traveled: Testing: $F_{(2,53)} = 1.363$, $p = 0.2646$; Reversal: $F_{(2,53)} = 0.1803$, $p = 0.8355$) (Fig. 2F; Supplementary Fig. 1B).

Overall, these data suggest that, although 6-month-old 3xTg-AD + EtOH mice tend to have the poorest performance during the testing and reversal phases of the Barnes maze task, the differences are less dramatic at 6 months than at 4 months of age. These findings are consistent with the notion of a precocious appearance of spatial memory deficits without exacerbating their severity in 3xTg-AD mice exposed prenatally to ethanol.

Ethanol exposure results in age-dependent changes in glutamatergic and GABAergic synaptic inputs to Layer V/VI pyramidal neurons in the mPFC

Synaptic loss and dysfunction precede the onset of the protein-based biomarkers of AD and have been reported to be more predictive of cognitive performance than levels of tau or β-amyloid deposition (Arendt, 2009; DeKosky & Scheff, 1990; Scheff, Price, Schmitt, & Mufson, 2006; Selkoe, 2002). Our ethanol exposure paradigm results in altered synaptic connectivity in the mPFC of young adult mice (Skorput et al., 2015). Thus, we sought to determine whether there were differences in synaptic function between B6129, 3xTg-AD, and 3xTg-AD + EtOH mice. We recorded spontaneous postsynaptic glutamatergic (sEPSC) and GABAergic (sIPSC) currents from layer V/VI pyramidal neurons in the mPFC of the same 4-month-old and 6-month-old mice that were tested behaviorally. Pyramidal neurons were identified online under Hoffman Modulation Contrast optics based on their laminar location and large size of the cell bodies relative to neighboring cells. Their morphology was also confirmed *post hoc* following intracellular filling with neurobiotin (Fig. 3A). Glutamatergic and GABAergic sPSCs were isolated from individual cells by recording at holding potentials of −70 mV and 0 mV, respectively, and analyzed separately by age to explore the effects of prenatal ethanol on the onset vs. progression of AD-related changes in synaptic transmission.

Both mean sEPSC and sIPSC frequency were significantly affected in pyramidal neurons recorded in the mPFC of 4-month-old mice (one-way ANOVA, sEPSC frequency: $F_{(2,40)} = 4.702$, $p = 0.0147$; sIPSC frequency: $F_{(2,40)} = 3.842$, $p = 0.0298$). However, only sIPSC frequency was significantly affected at 6 months of age (one-way ANOVA, sEPSC frequency: $F_{(2,40)} = 1.984$, $p = 0.1523$; sIPSC frequency: $F_{(2,40)} = 5.822$, $p = 0.0063$) mice (Figs. 3C, 4A, 5A, and 6A). Bonferroni *post hoc* tests indicated that cells from 4-month-old 3xTg-AD + EtOH mice displayed decreased sEPSC frequency and a distinct rightward shift in the cumulative frequency distribution, reflecting increased inter-stimulus interval (sEPSC frequency: 4.649 ± 0.8420 Hz) relative to those recorded from B6129 mice (sEPSC frequency: 8.044 ± 1.110 Hz, $t = 2.517$, $p < 0.05$) and 3xTg-AD mice (sEPSC frequency: 8.356 ± 0.9183 Hz, $t = 2.749$, $p < 0.05$) (Fig. 3A). sIPSC frequency differed between cells from 4-month-old B6129 and 3xTg-AD + EtOH mice, with cells from 3xTg-AD + EtOH mice showing a decrease in frequency and a rightward shift in the cumulative distribution of interstimulus interval (B6129: 8.766 ± 0.8418 Hz; 3xTg-AD + ETOH: 5.973 ± 0.5527 Hz, $t = 2.758$, $p < 0.05$). sEPSC and sIPSC frequency did not differ in cells recorded from 3xTg-AD (sEPSC frequency: 8.356 ± 0.9183; sIPSC frequency: 7.570 ± 0.7561 Hz) and B6129 mice (sEPSC frequency: 8.044 ± 1.110 Hz; sIPSC frequency: 8.766 ± 0.8418 Hz) (Fig. 4A).

In the mPFC of 6-month-old 3xTg-AD + EtOH mice, Layer V/VI pyramidal neurons trended toward decreased sEPSC frequency (3.889 ± 09879 Hz) relative to B6129 (5.962 ± 0.9879 Hz) and 3xTg-AD mice (6.433 ± 0.1.028 Hz), but did not reach statistical significance (Fig. 5A). sIPSC frequency significantly decreased in 3xTg-AD and 3xTg-AD + EtOH mice (5.692 ± 0.6343 Hz and 5.23 ± 0.8729 Hz, respectively) relative to those monitored in 6-month-old B6129 mice (9.055 ± 0.9925 Hz) (Fig. 6A). These data suggest an age-dependent diminution of presynaptic GABAergic, but not glutamatergic, inputs to mPFC pyramidal neurons in 3xTg-AD mice at both 4 and 6 months of age (Supplementary Fig. 4).

Experimental condition significantly affected mean sIPSC amplitude in 4-month-old mice (one-way ANOVA, $F_{(2,40)} = 5.788$, $p = 0.0063$), with cells from 3xTg-AD mice demonstrating an increase in sIPSC amplitude and leftward shift in the cumulative distribution of amplitude relative to cells recorded from both B6129 and 3xTg-AD + EtOH mice (Bonferroni *post hoc*, 3xTg-AD vs. B6129: $t = 2.903$, $p < 0.05$; 3xTg-AD vs. 3xTg-AD + EtOH: $t = 2.989$, $p < 0.05$) (Fig. 4B). By 6 months of age, though sIPSCs amplitudes recorded from 3xTg-AD mice tended to be larger (16.35 ± 1.380 pA), differences from B6129 (12.53 ± 0.5269 pA) and 3xTg-AD + EtOH (12.49 ± 0.6462 pA) mice were no longer significant (Kruskall–Wallis test, $p = 0.0610$) (Fig. 6B). sEPSC amplitude did not differ in cells from either 4-month-old (B6129: 8.871 ± 0.4151; 3xTg-AD: 9.697 ± 0.5884 pA; 3xTg-AD + ETOH: 8.808 ± 0.2695 pA) or 6-month-old mice (B6129: 8.539 ± 0.4814 pA; 3xTg-AD: 8.526 ± 0.4833 pA; 3xTg-AD + ETOH: 8.76 ± 0.5294 pA) (one-way ANOVA, 4-month-old: $F_{(2,40)} = 1.276$, $p = 0.2903$; 6-month-old: $F_{(2,40)} = 0.070$, $p = 0.9329$) (Figs. 3D and 5B). The increase in sIPSC amplitude in 3xTg-AD mice relative to B6129 and 3xTg-AD + EtOH mice suggests that prenatal ethanol exposure may prevent layer V/VI pyramidal neurons in 3xTg-AD mice from compensating for presynaptic deficits related to AD pathology with an increase in the number or function of postsynaptic GABAergic receptors.

Experimental condition also significantly affected the mean sEPSC charge in layer V/VI mPFC pyramidal neurons from 4-month-old mice (Kruskall–Wallis test, $p < 0.0001$). Layer V/VI pyramidal neurons recorded from 4-month-old 3xTg-AD + EtOH mice displayed a significant increase in charge relative to those from 3xTg-AD mice and B6129 mice (3xTg-AD + EtOH:, 36.67 ± 2.497 pA·ms; 3xTg-AD: 23.03 ± 2.497 pA·ms; B6: 19.65 ± 2.110 pA·ms; Dunn's multiple comparison test, B6129 vs. 3xTg-AD + EtOH, $p < 0.001$; 3xTg-AD vs. 3xTg-AD + EtOH, $p < 0.01$). This increase in charge was associated with significant increases in both rise and decay time in cells from 4-month-old 3xTg-AD + EtOH mice (rise time:

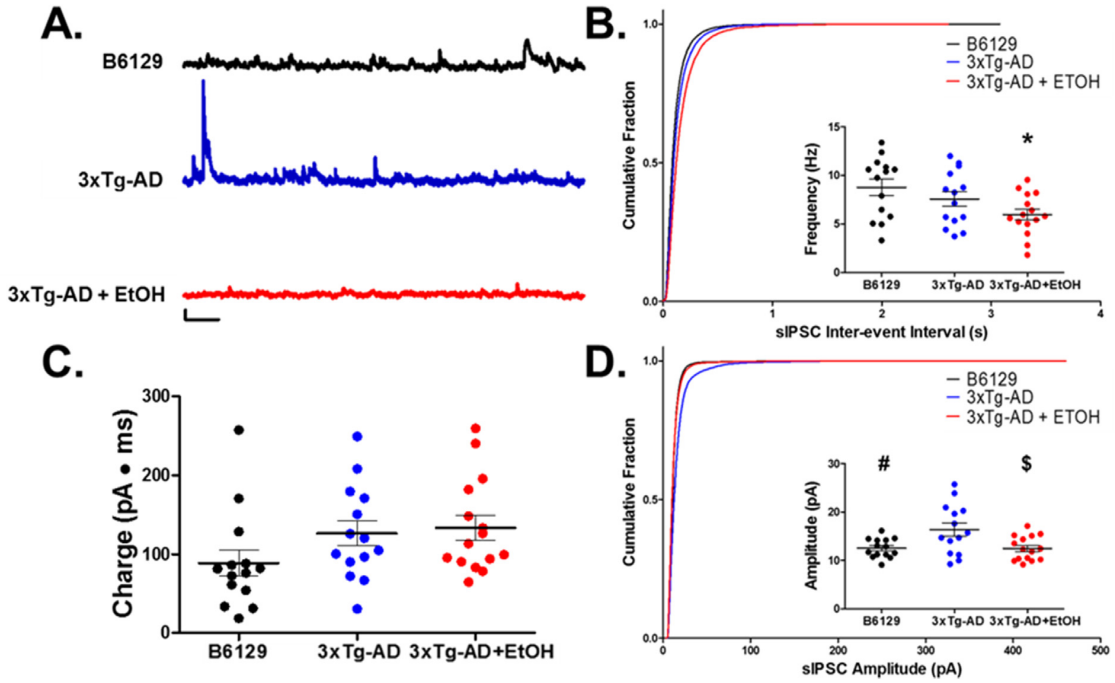

Fig. 4. Prenatal ethanol exposure decreases the frequency of spontaneous inhibitory post-synaptic currents (sIPSCs) in the medial prefrontal cortex (mPFC) of 4-month-old 3xTg-AD mice. (**A**) Representative traces of whole-cell voltage clamp recordings of sIPSCs recorded at a holding potential 0 mV from Layer V/VI pyramidal neurons in acute mPFC slices from 4-month-old: B6129 (black), 3xTg-AD (blue), and 3xTg-AD + EtOH (red) mice; scale bar = 250 ms × 20 pA. (**B**) Cumulative distribution of sIPSC inter-event intervals (s) recorded Layer V/VI pyramidal neurons of 4-month-old: B6129 (black), 3xTg-AD (blue), and 3xTg-AD + EtOH (red) mice. (inset): Mean sIPSC frequency of Layer V/VI pyramidal neurons of mPFC of 4-month-old: B6129 (black dots), 3xTg-AD (blue dots), and 3xTg-AD + EtOH (red dots) mice. (**C**) Cumulative distribution of sIPSC amplitude intervals (s) recorded from Layer V/VI pyramidal neurons of 4-month-old B6129 (black), 3xTg-AD (blue), and 3xTg-AD + EtOH (red) mice. (inset): Mean sIPSC amplitude of Layer V/VI pyramidal neurons of mPFC of 4-month-old: B6129 (black dots), 3xTg-AD (blue dots), and 3xTg-AD + EtOH mice (red dots). (**D**) Mean sIPSC amplitude of Layer V/VI pyramidal neurons of mPFC of 4-month-old: B6129 (black dots), 3xTg-AD (blue dots), and 3xTg-AD + EtOH (red dots) mice. (**B**) * = $p < 0.05$, B6129 vs. 3xTg-AD + EtOH, one-way ANOVA with Bonferroni *post hoc* tests. (**D**) # = $p < 0.05$, 3xTg-AD vs. B6129, $ = $p < 0.05$, 3xTg-AD vs. 3xTg-AD + EtOH, one-way ANOVA with Bonferroni *post hoc* tests. For all measures: B6129 ($N = 14$ cells, $n = 4$ F, 5 M, 6 litters), 3xTg-AD ($N = 15$ cells, $n = 5$ F, 5 M, 6 litters), and 3xTg-AD + ETOH ($N = 15$ cells, $n = 3$ F, 7 M, 7 litters). N = total number of cells per group (dots) from n = total number mice by sex: F (female), M (male).

2.887 ± 0.1267 ms; decay time: 2.981 ± 0.1817 ms) relative to those from B6129 mice (rise time: 1.946 ± 0.1771 ms; decay time: 1.644 ± 0.1843 ms) and 3xTg-AD mice (rise time: 2.160 ± 0.1764 ms; decay time: 1.798 ± 0.1484 ms), while sEPSC amplitude was unaffected by experimental conditions at 4 months of age (one-way ANOVA, rise time: $F_{(2,40)} = 1.364$, $p = 0.2683$; decay time: $F_{(2,40)} = 2.428$, $p = 0.1160$; amplitude: $F_{(2,40)} = 1.276$, $p = 0.2903$) (Fig. 3D and Supplementary Figs. 2A and B). No group-dependent effects were observed in sIPSC charge at 4 months (one-way ANOVA, $F_{(2,40)} = 1.364$, $p = 0.1190$), nor sEPSC or sIPSC charge at 6 months of age (Kruskall–Wallis test, sEPSC charge: $p = 0.0625$, one-way ANOVA; sIPSC charge: $p = 0.0574$) (Figs. 4C, 5C and 6C). The differences in mean glutamatergic and GABAergic frequency, amplitude, and charge were not accompanied by changes in the overall excitatory:inhibitory ratio at either the 4-month or 6-month timepoints (one-way ANOVAs, 4-month-old: frequency: $F_{(2,40)} = 2.512$, $p = 0.0938$; amplitude: $F_{(2,40)} = 1.856$, $p = 0.1679$; charge: $F_{(2,40)} = 1.480$, $p = 0.2398$; 6-month-old: frequency: $F_{(2,40)} = 2.102$, $p = 0.1366$; amplitude: $F_{(2,40)} = 3.079$, $p = 0.0579$; charge: $F_{(2,40)} = 0.8732$, $p = 0.4260$) (Supplementary Fig. 3).

Our results suggest that prenatal ethanol exposure hastens the onset of deficits in presynaptic GABAergic inputs to Layer V/VI pyramidal neurons in the mPFC of 3xTg-AD mice (Supplementary Fig. 4). In addition, ethanol-exposed 3xTg-AD + EtOH mice lack the postsynaptic changes to GABAergic synapses observed in 3xTg-AD mice. The changes to GABAergic synaptic properties coincided with a decrease in glutamatergic synaptic inputs.

3xTg-AD mice exposed prenatally to ethanol have fewer PV+ GABAergic interneurons in the mPFC

Given the decrease in GABAergic synaptic inputs to Layer V/VI mPFC pyramidal neurons in 3xTg-AD + EtOH mice, we next asked whether the number of GABAergic interneurons in the mPFC might be affected by AD genotype and whether the differences would be exacerbated by prenatal exposure to ethanol. We focused our assessment on parvalbumin-expressing (PV+) GABAergic interneurons that play an essential role in cortical network activity and cognitive function (Nahar, Delacroix, & Nam, 2021). GABAergic interneurons are susceptible to both AD pathology and prenatal ethanol exposure (Bird, Taylor, Pinkowski, Chavez, & Valenzuela, 2018; Cuzon et al., 2008; Madden et al., 2020; Marguet et al., 2020; Skorput et al., 2015; Xu, Zhao, Han, & Zhang, 2020). In this light, we assessed the disposition of PV+ interneurons in the mPFC of 4- and 6-month-old behaviorally tested B6129, 3xTg-AD, and 3xTg-AD + EtOH mice.

Both AD transgenes and prenatal ethanol exposure significantly decreased the number of PV+ GABAergic interneurons in 4-month-old mice (one-way ANOVA $F_{(2,21)} = 8.426$, $p < 0.01$). While a 29.1% decrease in the number of PV+ GABAergic interneurons was observed in 4-month-old 3xTg-AD mice (83.10 ± 8.1 cells) when compared to their B6129 counterparts (117.3 ± 12.4 cells; Bonferroni *post hoc*, $t = 2.668$, $p < 0.05$), 3xTg-AD + EtOH mice displayed an even more dramatic decrease of more than 50% of PV+ cells (58.52 ± 5.3 cells; Bonferroni *post hoc*, $t = 4.025$, $p < 0.01$) (Fig. 7B).

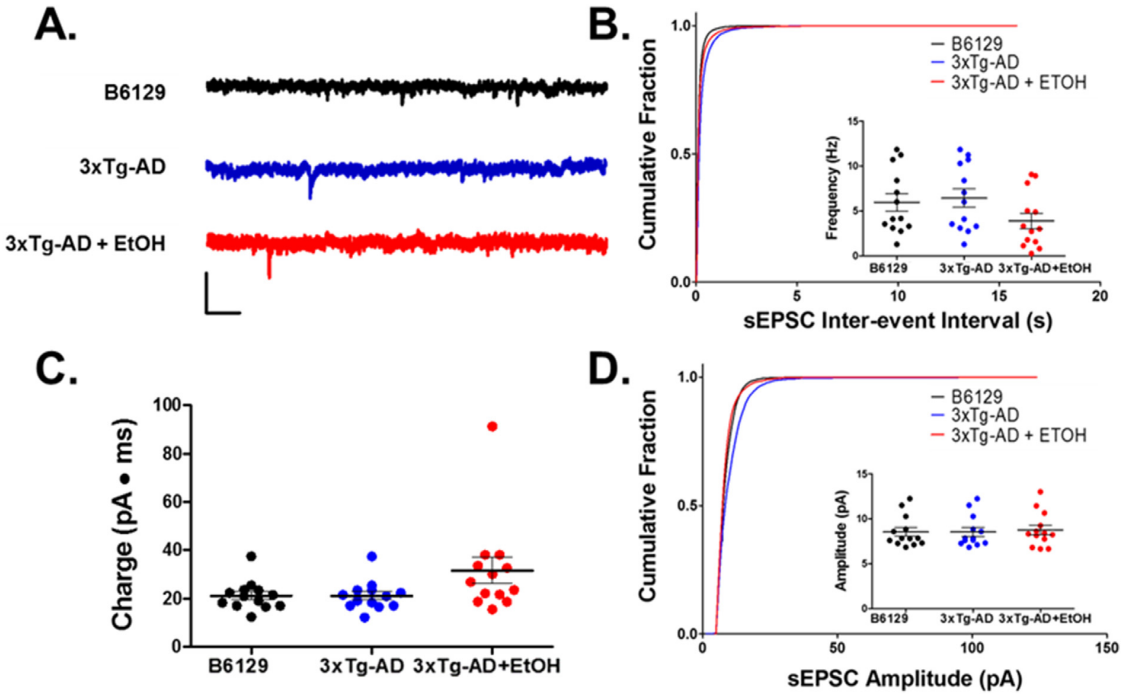

Fig. 5. Prenatal ethanol exposure does not alter the frequency, amplitude, or charge of spontaneous excitatory post-synaptic currents (sEPSCs) in the medial prefrontal cortex (mPFC) of 6-month-old 3xTg-AD mice. (**A**) Representative traces of whole-cell voltage clamp recordings of sEPSCs recorded at a holding potential −70 mV from Layer V/VI pyramidal neurons in acute mPFC slices from 6-month-old: B6129 (black), 3xTg-AD (blue), and 3xTg-AD + EtOH (red) mice. (**B**) Cumulative distribution of sEPSC inter-event intervals (s) recorded from Layer V/VI pyramidal neurons of 6-month-old: B6129 (black), 3xTg-AD (blue), and 3xTg-AD + EtOH (red). (inset): Mean sEPSC frequency of Layer V/VI pyramidal neurons of mPFC of 6-month-old: B6129 (black dots), 3xTg-AD (blue dots), and 3xTg-AD + EtOH (red dots) mice. (**C**) Cumulative distribution of sEPSC amplitude intervals (s) recorded Layer V/VI pyramidal neurons of 6-month-old: B6129 (black), 3xTg-AD (blue), and 3xTg-AD + EtOH mice (red). (inset): Mean sEPSC amplitude of Layer V/VI pyramidal neurons of mPFC of 6-month-old B6129 (black dots), 3xTg-AD (blue dots), and 3xTg-AD + EtOH (red dots) mice. (**D**) Mean sEPSC amplitude of Layer V/VI pyramidal neurons of mPFC of 6-month-old: B6129 (black dots), 3xTg-AD (blue dots), and 3xTg-AD + EtOH (red dots) mice. For all measures: B6129 (N = 13 cells, n = 4 F, 4 M, 5 litters), 3xTg-AD (N = 13 cells, n = 4 F, 6 M, 3 litters), and 3xTg-AD + ETOH (N = 14 cells, n = 4 F, 6 M, 5 litters). N = total number of cells per group (dots) from n = total number mice by sex: F (female), M (male).

By 6 months of age, both 3xTg-AD (59.4 ± 5.3 cells, 24.2% decrease) and 3xTg-AD + EtOH (50.71 ± 4.8 cells, 35.3% decrease) mice displayed decreases in PV+ GABAergic interneurons relative to B6129 mice at 4 months (78.4 ± 9.6 cells; one-way ANOVA, $F_{(2,21)} = 4.514$, $p < 0.05$). Differences at 6 months of age were less pronounced, with only 3xTg-AD + EtOH mice displaying significant differences relative to control mice (Bonferroni *post hoc*, $t = 2.974$, $p < 0.05$) (Fig. 8A and B).

Our findings point to an earlier decrease in the number of PV+ GABAergic interneurons in the mPFC of 3xTg-AD mice exposed prenatally to ethanol. In addition, while the control B6129 mice demonstrated a 33% loss of PV+ GABAergic interneurons in the mPFC between 4 and 6 months of age (Bonferroni *post hoc*, $t = 3.247$, $p < 0.01$), this age-dependent decrease is not significant in the 3xTg-AD (28.5% decrease) and 3xTg-AD + EtOH (13.3% decrease) mice (Supplementary Fig. 4).

Prenatal ethanol exposure results in region-specific and cortical layer-specific decreases in PV+ GABAergic interneurons in 3xTg-AD mice

Different layers and regions of the mPFC differ dramatically in cell composition and function, and afferent and efferent connections (Anastasiades & Carter, 2021). To assess whether AD pathology and the effects of prenatal ethanol exposure on the number of PV+ GABAergic interneurons in the mPFC might be specific to a particular cortical layer (Layer I, II/II, V, or VI), or region (anterior cingulate [ACC], prelimbic [PL], and infralimbic [IL]), as identified by DAPI counterstaining, we first performed a three-way ANOVA with experimental group, region, and layer as factors. We identified a significant experimental group × layer × region interaction ($F_{(30,504)} = 11.196$, $p < 0.05$). Thus, cortical layer-specific differences were assessed in each region of the mPFC at 4 months and 6 months using two-way ANOVAs with group and layer as factors.

A significant effect of experimental group was found in the PL and IL regions of the mPFC in 4-month-old mice (PL: $F_{(2,84)} = 7.338$, $p = 0.0012$; IL: $F_{(2,84)} = 14.46$, $p < 0.0001$), but not in the ACC ($F_{(2,84)} = 2.199$, $p = 0.1173$). Bonferroni *post hoc* analyses of 4-month-old mice revealed significant differences in Layer V of the IL region between both 3xTg-AD (7.608 ± 1.075 cells, $t = 3.450$, $p < 0.01$) and 3xTg-AD + EtOH (6.333 ± 1.537 cells, $t = 3.896$, $p < 0.001$) relative to B6129 mice (12.07 ± 1.668 cells). Similarly, at 4 months, there were significantly fewer cells in Layer VI of the IL region in both 3xTg-AD (5.219 ± 0.88 cells, $t = 2.658$, $p < 0.05$) and 3xTg-AD + EtOH (4.567 ± 1.061 cells, $t = 2.778$, $p < 0.05$) relative to B6129 controls (8.657 ± 1.243 cells) (Fig. 7C). Significant differences were also observed between 4-month-old B6129 and 3xTg-AD + ETOH mice in Layer II/III of the ACC (B6129: 29.52 ± 10.05 cells; 3xTg-AD + EtOH: 13.82 ± 5.135 cells, $t = 2.577$, $p < 0.05$), PL (B6129: 15 ± 3.933 cells; 3xTg-AD + EtOH: 7.517 ± 2.256 cells, $t = 2.840$, $p < 0.05$), and IL (B6129: 7.235 ± 0.6739 cells; 3xTg-AD + EtOH: 3.45 ± 0.8902 cells, $t = 2.571$, $p < 0.05$) as well as Layer V of the PL regions (B6129: 14.08 ± 1.976 cells; 3xTg-AD + EtOH: 7.233 ± 1.575, $t = 2.598$, $p < 0.05$) (Fig. 7C).

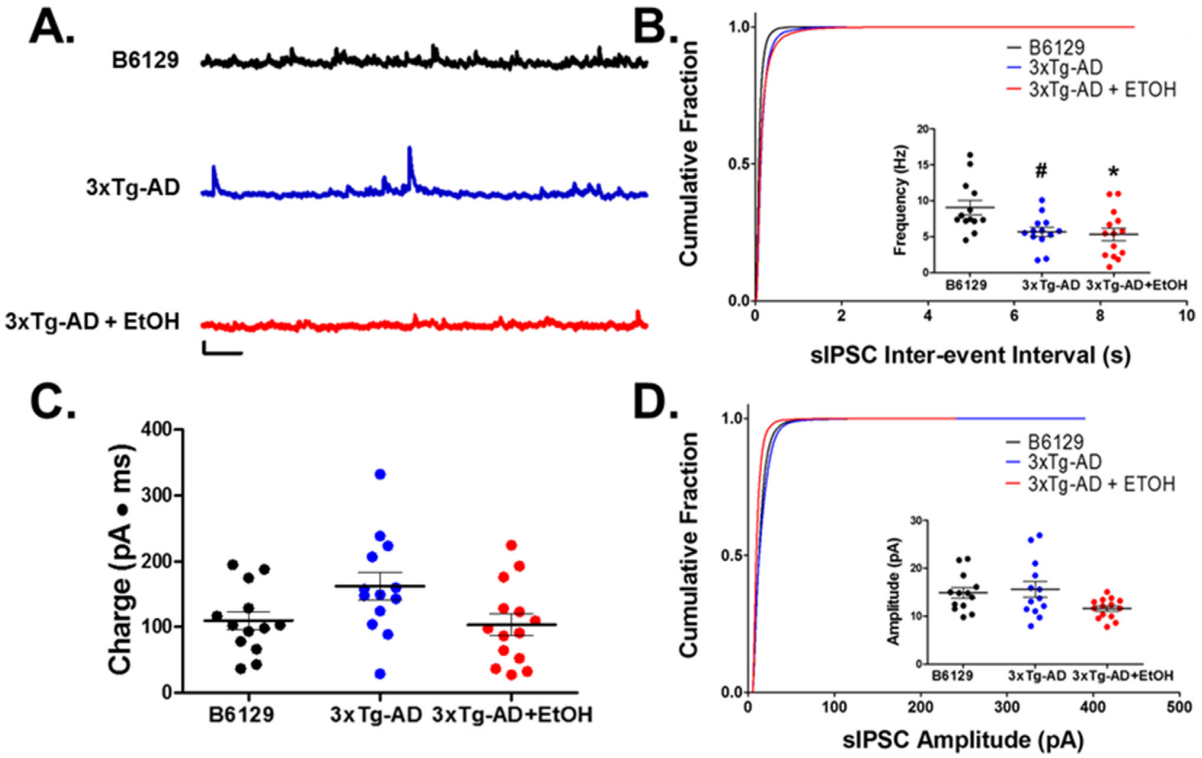

Fig. 6. Prenatal ethanol exposure decreases the frequency of spontaneous inhibitory post-synaptic currents (sIPSCs) in the medial prefrontal cortex (mPFC) of 6-month-old 3xTg-AD mice. (**A**) Representative traces of whole-cell voltage clamp recordings of sIPSCs recorded at a holding potential 0 mV from Layer V/VI pyramidal neurons in acute mPFC slices from 6-month-old: B6129 (black), 3xTg-AD (blue), and 3xTg-AD + EtOH (red). (**B**) Cumulative distribution of sIPSC inter-event intervals (s) recorded from Layer V/VI pyramidal neurons of 6-month-old: B6129 (black), 3xTg-AD (blue), and 3xTg-AD + EtOH (red) mice, (inset): Mean sIPSC frequency of Layer V/VI pyramidal neurons of mPFC of 6-month-old: B6129 (black dots), 3xTg-AD (blue dots), and 3xTg-AD + EtOH (red dots) mice. (**C**) Cumulative distribution of sIPSC amplitude intervals (s) recorded Layer V/VI pyramidal neurons of 6-month-old: B6129 (black), 3xTg-AD (blue), and 3xTg-AD + EtOH mice (red). (inset): Mean sIPSC amplitude of Layer V/VI pyramidal neurons of mPFC of 6-month-old: B6129 (black dots), 3xTg-AD (blue dots), and 3xTg-AD + EtOH (red dots) mice. (**D**) Mean sIPSC amplitude of Layer V/VI pyramidal neurons of mPFC of 6-month-old: B6129 (black dots), 3xTg-AD (blue dots), and 3xTg-AD + EtOH mice (red dots). (**B**) # = $p < 0.05$, 3xTg-AD vs. B6129, * = $p < 0.05$, B6129 vs. 3xTg-AD + EtOH, one-way ANOVA with Bonferroni *post hoc* tests. (**D**) ### = $p < 0.001$, 3xTg-AD vs. B6129, $$$ = $p < 0.001$, 3xTg-AD vs. 3xTg-AD + EtOH, one-way ANOVA with Bonferroni *post hoc* tests. For all measures: B6129 ($N = 13$ cells, $n = 4$ F, 4 M, 5 litters), 3xTg-AD ($N = 13$ cells, $n = 4$ F, 6 M, 3 litters), and 3xTg-AD + ETOH ($N = 14$ cells, $n = 4$ F, 6 M, 5 litters). N = total number of cells per group (dots) from n = total number mice by sex: F (female), M (male).

In 6-month-old mice, consistent with observations in their 4-month-old counterparts, a significant effect of experimental group was observed only in the PL and IL mPFC regions (PL: $F_{(2,84)} = 11.18$, $p < 0.0001$; IL: $F_{(2,84)} = 9.577$, $p = 0.0002$). Again, no differences were observed between groups in the ACC ($F_{(2,84)} = 2.004$, $p = 0.1412$). *Post hoc* analyses identified differences between both 3xTg-AD and 3xTg-AD + EtOH mice relative to B6129 controls in Layers V and VI of the PL mPFC (Layer V, B6129: 12.74 ± 2.146 cells; 3xTg-AD: 8.175 ± 1.095 cells; 3xTg-AD + EtOH: 7.7 ± 0.9245; B6129 vs. 3xTg-AD: $t = 3.578$, $p < 0.01$; B6129 vs. 3xTg-AD + EtOH: $t = 4.067$, $p < 0.001$; Layer VI, B6129: 8.829 ± 0.9564 cells; 3xTg-AD: 5.425 ± 0.4617 cells; 3xTg-AD + EtOH: 5.256 ± 0.5242 cells; B6129 vs. 3xTg-AD: $t = 2.673$, $p < 0.05$; B6129 vs. 3xTg-AD + EtOH: $t = 2.882$, $p < 0.05$) (Fig. 8C). Differences specific to 3xTg-AD + EtOH vs. B6129 mice were observed in Layer V and VI of IL mPFC (Layer V, B6129: 12.86 ± 1.724 cells; 3xTg-AD + EtOH: 7.289 ± 1.386 cells, $t = 4.060$, $p < 0.001$; Layer VI, B6129: 10.96 ± 1.2 cells; 3xTg-AD + EtOH: 6.056 ± 1.109 cells, $t = 3.574$, $p < 0.01$) (Fig. 8C).

Overall, 3xTg-AD mice displayed a trend toward decreased PV+ interneurons in the PL and IL of the mPFC independent of prenatal ethanol exposure. However, with prenatal ethanol exposure, the decrease in PV+ interneurons was more widespread and severe, particularly in the deeper layers V and VI in the mPFC of 3xTg-AD mice. These differences were most apparent in 4-month-old mice, whereas fewer regions were affected in 3xTg-AD + EtOH mice at 6 months.

Prenatal ethanol exposure results in an earlier onset of β-amyloid pathology in 3xTg-AD mice

Pathological accumulation of β-amyloid and tau proteins coincides with the development of GABAergic interneuron dysfunction in animal models of AD and in human AD patients (Ali, Baringer, Neal, Choi, & Kwan, 2019; Li et al., 2016; Tampellini, 2015). In 3xTg-AD mice, accumulation of intraneuronal β-amyloid occurs by 4 months of age, coinciding with onset of cognitive deficits and preceding the formation of amyloid plaques by 6 months of age, as well as the onset of pathological tau neurofibrillary tangles, the latter not detected until 12–18 months of age (Billings et al., 2005; España et al., 2010). Here we asked whether PAE altered the accumulation of intraneuronal β-amyloid pathology in 4-month-old and 6-month-old 3xTg-AD mice. We measured the relative intensity of APP/Aβ immunofluorescence with 6E10, a mouse monoclonal antibody to human APP/Aβ driven by transgene expression.

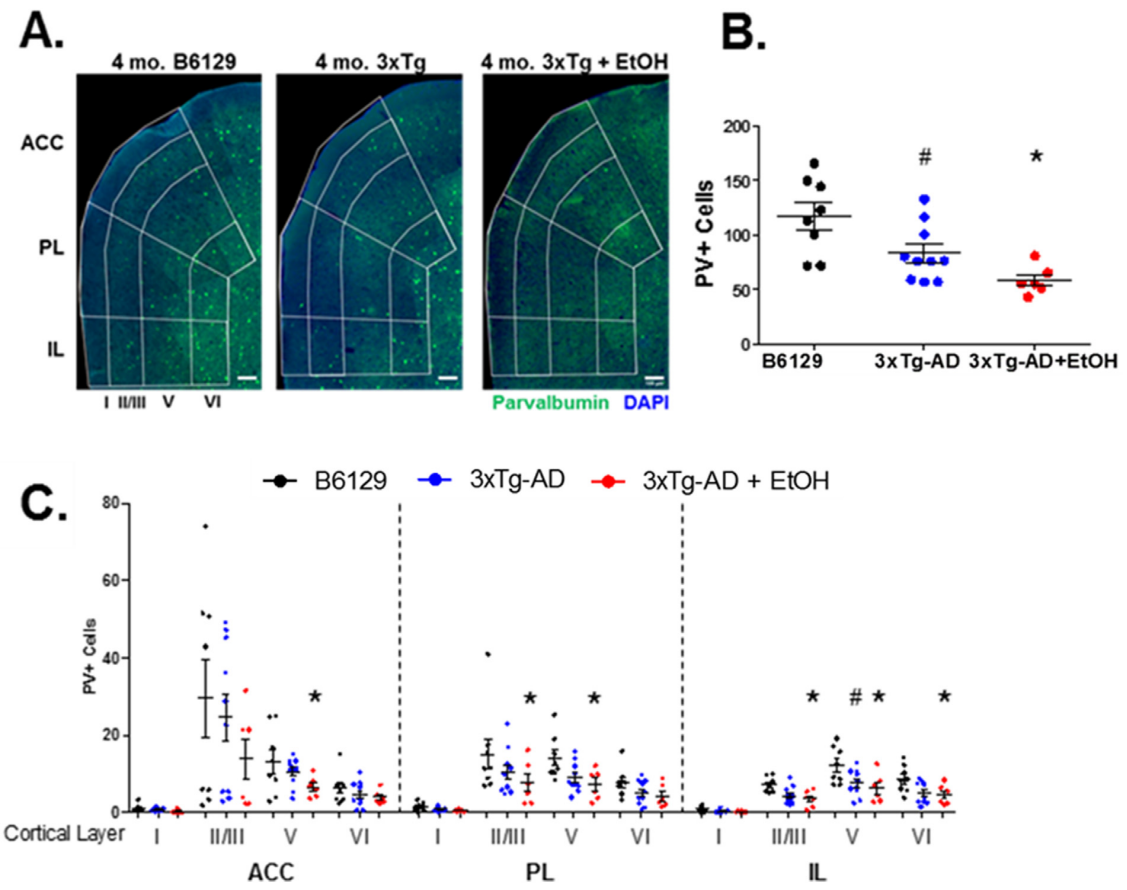

Fig. 7. Prenatal ethanol exposure results in more widespread diminution of parvalbumin immunoreactive (PV+) GABAergic interneurons in the medial prefrontal cortex (mPFC) of 4-month-old 3xTg-AD mice. (**A**) Example PV+ cells (green) in coronal sections of mPFC of 4-month-old: B6129, 3xTg-AD, and 3xTg-AD + EtOH mice with DAPI-counterstain (blue); scale bar = 100 μM. White lines demarcate the cortical layers: I, II/III, V, VI and subregions of the mPFC: anterior cingulate cortex (ACC), prelimbic cortex (PL), infralimbic cortex (IL). (**B**) Total number of PV+ cells in the mPFC of 4-month-old: B6129 (black dots), 3xTg-AD (blue dots), and 3xTg-AD + EtOH mice (red dots). (**C**) Number of PV+ cells in layers I, II/II, V, and VI of the ACC, PL, and IL regions of the mPFC of 4-month-old: B6129 (black dots), 3xTg-AD (blue dots), and 3xTg-AD + EtOH (red dots) mice. (**B**) # = $p < 0.05$ B6129 vs. 3xTg-AD, * = $p < 0.05$ B6129 vs. 3xTg-AD + EtOH, one-way ANOVA with Bonferroni *post hoc* tests. (**C**) # = $p < 0.05$ B6129 vs. 3xTg-AD, * = $p < 0.05$ B6129 vs. 3xTg-AD + EtOH, two-way ANOVA with Bonferroni *post hoc* tests. For all measures: B6129 ($N = 8$ brains, $n = 4$ F, 4 M, 5 litters), 3xTg-AD ($N = 10$ brains, $n = 4$ F, 4 M, 5 litters), and 3xTg-AD + ETOH mice ($N = 6$ brains, $n = 3$ F, 3 M, 3 litters). N = total number of brains per group (dots) from n = total number brains by sex: F (female), M (male).

A two-way ANOVA with age and group as factors revealed a significant effect of group on APP/Aβ relative fluorescence intensity ($F_{(2,12)} = 10.49$, $p < 0.01$). In 4-month-old mice, *post hoc* analysis revealed both diffuse and intraneuronal APP/Aβ fluorescence in 3xTg-AD (0.1436 ± 0.0252) and 3xTg-AD + EtOH (0.1655 ± 0.010) mice. However, only 3xTg-AD + EtOH mice had significantly increased APP/Aβ fluorescence relative to B6129 animals (0.1094 ± 0.0174) (Bonferroni *post hoc*, B6129 vs. 3xTg-AD + EtOH: $t = 2.724$, $p < 0.05$). Alternatively, at 6 months of age, both 3xTg-AD (0.1738 ± 0.011) and 3xTg-AD + EtOH (0.1059 ± 0.007) mice showed significantly increased APP/Aβ fluorescence relative to B6129 animals (Bonferroni *post hoc*, B6129 vs. 3xTg-AD: $t = 3.303$, $p < 0.05$; B6129 vs. 3xTg-AD + EtOH: $t = 3.361$, $p < 0.05$). This again suggested that PAE may hasten the onset of AD phenotypes in 3xTG-AD mice. In addition, β-amyloid staining did not appear to co-localize with parvalbumin + GABAergic interneurons, consistent with previous reports that intraneuronal human β-amyloid is preferentially expressed in pyramidal neurons, likely due to Thy1.2 promoter-driven transgene expression in 3xTg-AD mice (España et al., 2010) (Supplementary Fig. 5).

Discussion

In this study, we provide the first preclinical evidence that prenatal ethanol exposure can contribute to AD pathology. Prenatal ethanol exposure alters developing neurocircuits and can result in differences in behavior and cognition in children that persist into adulthood (Delatour & Yeh, 2017; Jacobson et al., 2021; Wozniak et al., 2019). How prenatal ethanol exposure may contribute to neurocircuit-level and cognitive changes during aging in general, and specifically to the risk and/or progression of AD, is uncertain. The major finding of this study is that prenatal ethanol exposure resulted in a precocious onset of spatial memory deficits and reversal learning deficits in 4-month-old 3xTg-AD mice, while differences were less severe in 6-month-old mice. This is consistent with the notion that prenatal ethanol exposure may alter the onset but not the severity of AD symptoms. These changes coincided with age-dependent alterations in glutamatergic and GABAergic synaptic activity, as well as a progressive decrease in PV+ GABAergic interneurons and an accumulation of β-amyloid in the mPFC.

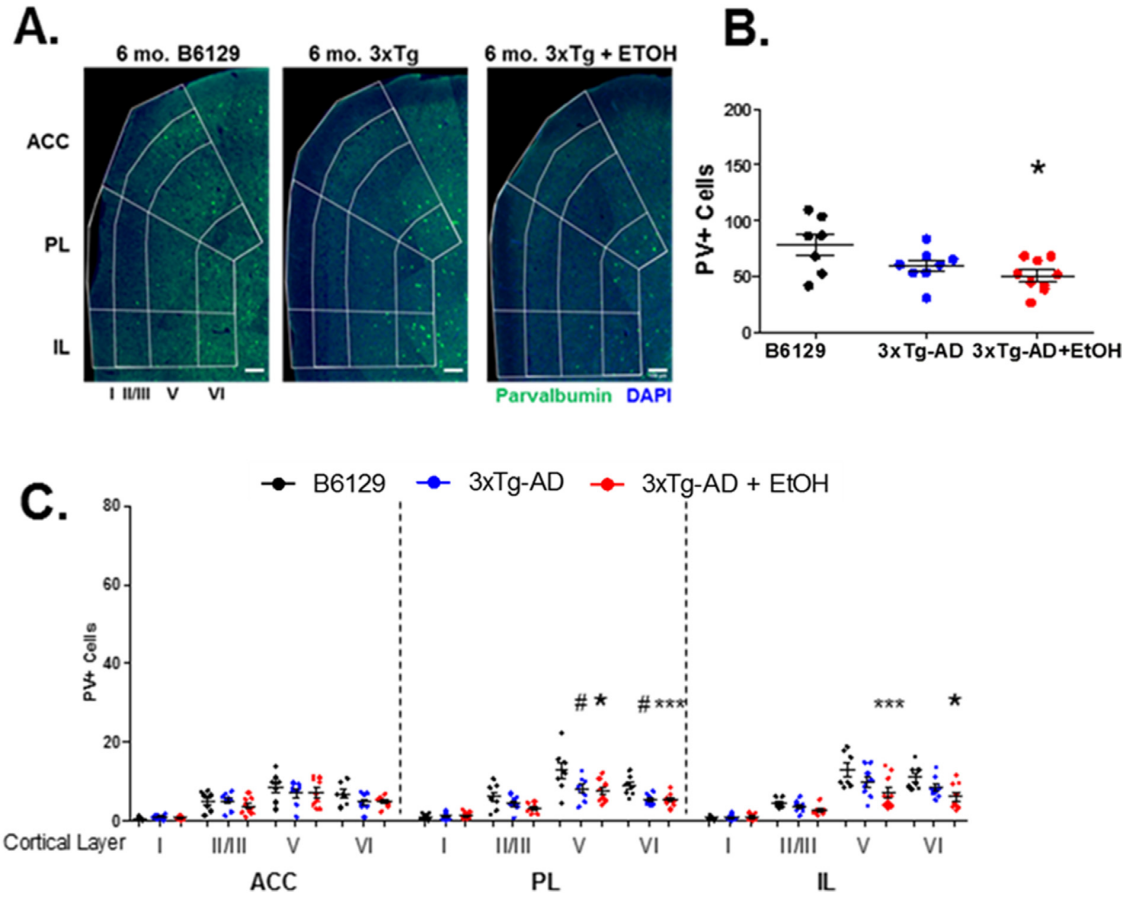

Fig. 8. Prenatal ethanol exposure results in layer-specific and region-specific diminution of immunoreactive (PV+) GABAergic interneurons in the medial prefrontal cortex (mPFC) of 6-month-old 3xTg-AD mice. (**A**) Example PV+ cells (green) in coronal sections of mPFC of 6-month-old: B6129, 3xTg-AD, and 3xTg-AD + EtOH mice with DAPI-counterstain (blue); scale bar = 100 μM. White lines demarcate the cortical layers: I, II/III, V, VI and subregions of the mPFC: anterior cingulate cortex (ACC), prelimbic cortex (PL), infralimbic cortex (IL). (**B**) Total number of PV+ cells in the mPFC of 6-month-old: B6129 (black dots), 3xTg-AD (blue dots), and 3xTg-AD + EtOH (red dots) mice. (**C**) Number of PV+ cells in layers I, II/II, V, and VI of the ACC, PL, and IL regions of the mPFC of 6-month-old: B6129 (black dots), 3xTg-AD (blue dots), and 3xTg-AD + EtOH mice (red dots). (**B**) * = $p < 0.05$ B6129 vs. 3xTg-AD + EtOH, one-way ANOVA with Bonferroni *post hoc* tests. (**C**) # = $p < 0.05$ B6129 vs. 3xTg-AD, * = $p < 0.05$, *** = $p < 0.001$ B6129 vs. 3xTg-AD + EtOH, two-way ANOVA with Bonferroni *post hoc* tests. For all measures: B6129 ($N = 7$ brains, $n = 4$ F, 3 M, 4 litters), 3xTg-AD ($N = 7$ brains, $n = 3$ F, 4 M, 4 litters), and 3xTg-AD + ETOH ($N = 7$ brains, $n = 4$ F, 5 M, 4 litters). N = total number of brains per group (dots) from n = total number brains by sex: F (female), M (male).

3xTg-AD mice exposed to ethanol in utero develop cognitive deficits earlier, but do not show differences in the progression or severity of the deficits

We demonstrated that while 4-month-old 3xTg-AD mice displayed some spatial memory deficits, 3xTg-AD + EtOH mice had more severe spatial memory impairment and behavioral flexibility. Alternatively, while 6-month-old 3xTg-AD + EtOH mice continued to perform the most poorly in the modified Barnes maze task, group-dependent differences in task performance were no longer significant. The lack of observed differences between B6129 and 3xTg-AD mice stands in contrast to previous work that demonstrated spatial memory deficits using the modified Barnes maze task in 6-month-old 3xTg-AD animals (Muñoz et al., 2015; Stover, Campbell, Van Winssen, & Brown, 2015). The more subtle differences between 6-month-old 3xTg-AD and 3xTg-AD + EtOH groups suggests that mice may employ different strategies at different ages that may account for the observed decrease in severity in spatial memory.

The potential for age-dependent differences in behavioral task strategy is supported by differences in the onset of cognitive deficits in 3xTg-AD mice, observed depending on the method of behavioral assessment and the type of cognition assessed (Billings et al., 2005; Clinton et al., 2007; Pietropaolo, Feldon, & Yee, 2008; Stevens & Brown, 2015). The possibility cannot be ruled out that prenatal ethanol exposure could have increased the severity of AD symptoms later in disease progression had we employed a different learning and memory behavioral paradigm. Indeed, given the continued progression of decrease in PV+ GABAergic interneurons, synaptic deficits, and subtle differences in spatial memory behavior in 6-month-old mice, future work should assess 3xTg-AD mice using more complex spatial memory tasks, testing alternate types of memory, and at older ages.

In addition, given the lack of observed differences in ethanol-exposed or ethanol-unexposed 6-month-old 3xTg-AD mice relative to control mice, or between 3xTg-AD and 3xTg-AD + EtOH groups at either time point, it is possible that the differences we observed in the modified Barnes maze task performance of 4-

month-old 3xTg-AD + EtOH mice represents an effect of prenatal ethanol exposure on cognition rather than a modification of the progression of AD pathology. Our past work suggests that young adult mice of a C57B6 background strain exposed prenatally to ethanol demonstrated reversal learning deficits but no alterations in spatial learning or memory on the modified Barnes maze task (Skorput et al., 2015). Prenatal ethanol exposure to mice of the B6129 background strain may result in spatial memory deficits in addition to reversal learning deficits in modified Barnes maze task performance, or alternatively memory deficits may appear in older adult animals exposed prenatally to ethanol regardless of background strain.

While strain differences in the physical effects of prenatal ethanol exposure have been observed, less is known about whether these differences alter cognitive and behavioral performance (Chen, Ozturk, Ni, Goodlett, & Zhou, 2011; Downing et al., 2009; Ogawa, Kuwagata, Ruiz, & Zhou, 2005). Future work should address whether strain differences extend to differences in spatial learning and memory, and alternatively explore the progression of cognitive differences in aging mice exposed prenatally to ethanol. However, given the parallels in age-related differences of 3xTg-AD and 3xTg-AD + EtOH mice relative to control mice, in cognitive performance, presence of synaptic dysfunction, changes in PV+ GABAergic interneuron numbers, and the degree of amyloid deposition, we believe it is likely that these cognitive deficits we observed in 4-month-old mice reflect an earlier onset of AD pathology (Fig. 9, Supplementary Fig. 5). Alternatively, employing a heavier binge or longer time course of prenatal ethanol exposure may amplify subtle differences we observed between 3xTg-AD and 3xTg-AD + EtOH mice.

Spatial memory deficits and behavioral inflexibility in ethanol-exposed 3xTg-AD mice coincide with age-dependent changes in synaptic connectivity

We found precocious progression of presynaptic GABAergic deficits in 3xTg-AD + EtOH mice. Dysfunction of inhibitory synapses has been reported in mouse models of AD as well as *post mortem* tissue from human AD patients (Kiss et al., 2016; Kurucu et al., 2021; Li et al., 2021; Mitew, Kirkcaldie, Dickson, & Vickers, 2013; Palop & Mucke, 2016; Prince et al., 2021; Verret et al., 2012). Conversely, recent work suggests that modifying GABAergic function can improve cognitive outcomes in mouse models of AD (Hijazi et al., 2019; Martinez-Losa et al., 2018). Several mechanisms could account for the differences in sPSC frequency, including change in the number of synapses, in the release probability of vesicles in response to changes in intracellular calcium levels, or in the number of vesicles present presynaptically. These may result from differences in action potential-driven or spontaneous vesicle release events (Ramirez & Kavalali, 2011). Both ethanol exposure and AD pathology have been shown to alter presynaptic function and intracellular calcium dynamics (Barthet & Mulle, 2020; Catlin, Guizzetti, & Costa, 1999; Lee, Yeh, & Yeh, 2022; Leslie, Brown, Dildy, & Sims, 1990; Lovinger, 2018; Siggins, Roberto, & Nie, 2005; Tong, Wu, Li, & Cheung, 2018). Our findings underscore the importance of considering changes in GABAergic interneuron function as a potential mechanism underlying early AD pathology in general, and specifically the effects of prenatal ethanol exposure on AD onset.

The enhanced postsynaptic GABA responses observed in 4-month-old 3xTg-AD mice are suggestive of increased postsynaptic receptor number or function. Altered postsynaptic GABA responses have been observed in young 3xTg-AD mice and other mouse models of AD (Chen et al., 2021; Hijazi et al., 2019; Li et al., 2021). Whether or not 3xTg-AD + EtOH mice develop postsynaptic GABAergic changes at earlier timepoints, and how postsynaptic changes may be affected at later timepoints, remains to be elucidated.

Changes in glutamatergic event kinetics could reflect alterations in composition of glutamate receptor subunits or glutamate receptor modulators (Hansen, Yuan, & Traynelis, 2007; Iacobucci & Popescu, 2018; Koike, Tsukada, Tsuzuki, Kijima, & Ozawa, 2000; Milstein & Nicoll, 2008; Stincic & Frerking, 2015). Both acute and chronic ethanol exposure have been shown to alter presynaptic glutamate release and glutamate receptor function in adult mice. However, further investigation into the mechanisms contributing to altered glutamatergic synaptic transmission in 3xTg-AD + EtOH is needed (Lovinger, 2018; Möykkynen & Korpi, 2012; Roberto et al., 2006; Roberto & Varodayan, 2017; Siggins et al., 2005). Overall, continued inquiry into the mechanisms underlying the pre- and post-synaptic changes in GABAergic and glutamatergic synaptic activity – could shed light on possible novel therapeutic targets for intervention at early stages of AD progression.

Altered GABAergic synaptic activity coincides with decreased number of PV+ GABAergic interneurons in ethanol-exposed 3xTg-AD mice

A diminution in PV+ GABAergic interneuron number and synaptic inputs was already present in 3xTg-AD mice at 4 months of age, but was more severe and widespread in 3xTg-AD + EtOH mice. It remains to be determined when changes in interneuron number first appear, and relatedly whether such changes are due to differences in the embryonic proliferation, migration of GABAergic interneurons in the mPFC, or the result of cell loss in adulthood. Migrating embryonic cortical neurons are susceptible to the effects of prenatal ethanol exposure (Cuzon et al., 2008; Delatour et al., 2019a; Lee et al., 2022; Skorput et al., 2015, 2019). Decreased numbers of GABAergic interneurons have also been identified in *post mortem* tissue from human AD patients (Arai, Emson, Mountjoy, Carassco, & Heizmann, 1987; Brady & Mufson, 1997; Sanchez-Mejias et al., 2020). In addition, several AD mouse models, including 3xTg-AD mice, have age-, region-, and mouse strain-dependent changes in interneuron number. As a case in point, loss of GABAergic interneurons in the hippocampus in particular has been associated with spatial memory deficits (Albuquerque et al., 2015; Andrews-Zwilling et al., 2010; Cheng et al., 2019; Leung et al., 2012; Murray et al., 2011; Sanchez-Mejias et al., 2020; Takahashi & Yamanaka, 2006; Verret et al., 2012). Neuroanatomical information regarding whether the loss of GABAergic interneurons in the 3xTg-AD mice is limited to the mPFC or may be manifest in other brain areas will provide insight into the pathological changes underlying observed spatial memory deficits.

Synaptic dysfunction and diminished numbers of PV+ GABAergic interneurons parallel increased accumulation of β-amyloid pathology in the mPFC of 3xTg-AD + EtOH mice

We observed an increased severity of β-amyloid pathology in 4-month-old 3xTg-AD mice exposed to ethanol when compared to unexposed animals. At 6 months of age, both 3xTg-AD and 3xTg-AD + EtOH mice demonstrated differences from control mice. Consistent with previous work, we observed the deposition of both diffuse and intraneuronal β-amyloid immunofluorescence in 4-month-old 3xTg-AD mice that appears to progress in 6-month-old mice regardless of ethanol exposure. These data provide further support for the hypothesis that prenatal ethanol exposure may modify the progression of AD phenotype in 3xTg-AD mice. Our findings also concur with work suggesting that prenatal stress can exacerbate early β-amyloid pathology in mouse models of AD (Jafari et al., 2019).

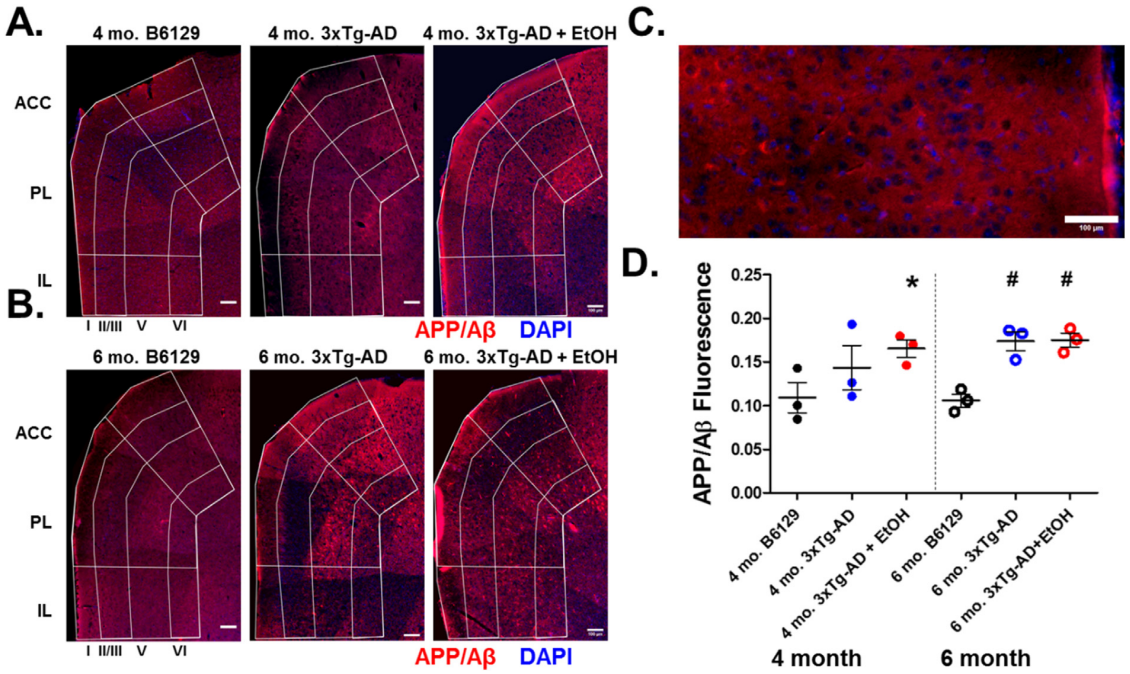

Fig. 9. Prenatal ethanol exposure increases amyloid precursor protein/beta amyloid (APP/Aβ) immunoreactivity in the medial prefrontal cortex (mPFC) of 4-month-old 3xTg-AD mice. (**A**) Representative images of APP/Aβ immunostaining (red) in coronal sections of mPFC of 4-month-old: B6129, 3xTg-AD, and 3xTg-AD + EtOH mice with DAPI-counterstain (blue); scale bar = 100 μM. White lines demarcate the cortical layers: I, II/III, V, VI and subregions of the mPFC: anterior cingulate cortex (ACC), prelimbic cortex (PL), infralimbic cortex (IL). (**C**) Example diffuse and intraneuronal APP/Aβ immunostaining (red) in Layers I–VI of the PL cortex of a 6-month-old 3xTg-AD + EtOH mPFC. (**D**) Relative APP/Aβ immunofluorescence intensity in the mPFC of 4-month-old: B6129 (filled black dots), 3xTg-AD (filled blue dots), and 3xTg-AD + EtOH (filled red dots) mice, and 6-month-old: B6129 (empty black dots), 3xTg-AD (empty blue dots), and 3xTg-AD + EtOH (empty red dots) mice. * = $p < 0.05$, 4-month-old B6129 vs. 4-month-old 3xTg-AD + EtOH, two-way ANOVA with Bonferroni *post hoc* tests, # = $p < 0.05$, 6-month-old B6129 vs. 6-month-old 3xTg-AD and 6-month-old B6129 vs. 6-month-old 3xTg-AD + EtOH. 4-month-old B6129 ($N = 3$ brains, $n = 1$ F, 2 M, 3 litters), 4-month-old 3xTg-AD ($N = 3$ brains, $n = 2$ F, 1 M, 3 litters), 4-month-old 3xTg-AD + ETOH ($N = 3$ brains, $n = 2$ F, 1 M, 2 litters), 6-month-old B6129 ($N = 3$ brains, $n = 2$ F, 1 M, 3 litters), 6-month-old 3xTg-AD ($N = 3$ brains, $n = 1$ F, 2 M, 3 litters), and 6-month-old 3xTg-AD + ETOH ($N = 3$ brains, $n = 1$ F, 2 M, 3 litters). N = total number of brains per group (dots) from n = total number brains by sex: F (female), M (male).

Intraneuronal β-amyloid accumulation has been demonstrated to precede that of phosphorylated tau and development of neurofibrillary tangles in the cortex of 3xTg-AD mice and *post mortem* brain tissue from individuals with AD (Oddo et al., 2003; Welikovitch et al., 2018). Intraneuronal β-amyloid deposition has been observed in the cortex of 3xTg-AD mice as young as 3 weeks old, while phosphorylated tau is not observed until animals reach 12 months of age (Billings et al., 2005; Oddo et al., 2003; Oh et al., 2010). Future work will address whether prenatal ethanol exposure alters the timing of onset or severity of tau pathology in older 3xTg-AD mice, and how this may be connected to the onset of β-amyloid pathology.

Progressive increases in intraneuronal β-amyloid have also been shown to coincide with the onset of cognitive deficits and synaptic dysfunction in several rodent models of AD (Billings et al., 2005; Chui et al., 1999; Gouras, Tampellini, Takahashi, & Capetillo-Zarate, 2010; Iulita et al., 2014; Leon et al., 2010; Takahashi et al., 2002). In considering how this accumulation of β-amyloid may relate to synaptic changes, diminution of GABAergic interneurons, and spatial memory performance of 3xTg-AD + EtOH mice, it is essential to consider when transgenic amyloid, presenilin, and tau proteins may first be present during development. The Thy1 promoter is first expressed embryonically in dividing neural precursor cells in the ventricular zone (Campsall et al., 2002; Caroni, 1997). However, reports vary in the developmental onset of Thy1-driven transgene expression (Campsall et al., 2002; Caroni, 1997). To begin to understand the complex relationship between network level dysfunction and β-amyloid proteinopathy in the 3xTg-AD model after prenatal ethanol exposure, it is prerequisite to determine when transgene expression, and related β-amyloid/tau pathology, are first detectable during development and how this may relate to the synaptic dysfunction as well as changes in cognition and behavioral flexibility later in life.

Implications in FASD

This study provided the first preclinical evidence of an association between prenatal alcohol exposure and AD risk. However, clinical and epidemiological studies have yet to explore how this may relate to the experiences of aging individuals with FASD. The clinical association between AD and other neurodevelopmental disorders, including autism spectrum disorder (ASD) and Down syndrome (DS), is already under investigation (Ballard, Mobley, Hardy, Williams, & Corbett, 2016; Head et al., 2003; Vivanti, Tao, Lyall, Robins, & Shea, 2021). It has been nearly 50 years since the first diagnosis of fetal alcohol syndrome (FAS), and appreciation of the diverse presentation of disorders with the FASD spectrum is still evolving and growing (Benz, Rasmussen, & Andrew, 2009; Jones & Smith, 1973; Wozniak et al., 2019). As increasing numbers of individuals with FASD begin to reach ages for assessing the onset of dementia and AD progression, further studies will enlighten and identify clinical needs to provide support throughout the aging process.

Conclusion

The experimental model and investigative approaches employed in this study provide a propitious opportunity to begin to understand how prenatal ethanol exposure may accelerate the onset of cognitive deficits in AD. Our findings reinforce the need to consider the long-term health outcomes of developmental exposures in general, and specifically the implications of *in utero* ethanol exposure on long-term cognitive function and AD risk.

Funding and declaration of interest

This work was supported by National Institutes of Health grants R01AG072900, R01AA027754 to HHY and F30AA029261 to ART.

Author contributions

HHY– Conceptualization, Supervision, Writing – review & editing; ART – Investigation, Data Curation, Formal Analysis, Writing – original draft; PWLY – Methodology, Investigation, Supervision, Writing – review and editing.

Acknowledgment

The authors thank Stephanie Lee for stimulating discussions related to mPFC structure and function and modified Barnes maze testing, and Dartmouth College undergraduates Zoe Enright, Avery Schuldt, Ryan Ding, Michelle Yu, and Megan Ungerman for their participation in preliminary data collection for neuroanatomical and behavioral experiments in this study.

Appendix A. Supplementary data

Supplementary data to this article can be found online at https://doi.org/10.1016/j.alcohol.2022.08.003.

References

Albuquerque, M. S., Mahar, I., Davoli, M. A., Chabot, J.-G., Mechawar, N., Quirion, R., et al. (2015). Regional and sub-regional differences in hippocampal GABAergic neuronal vulnerability in the TgCRND8 mouse model of Alzheimer's disease. *Frontiers in Aging Neuroscience, 7*, 30.

Ali, F., Baringer, S. L., Neal, A., Choi, E. Y., & Kwan, A. C. (2019). Parvalbumin-positive neuron loss and amyloid-β deposits in the frontal cortex of Alzheimer's disease-related mice. *Journal of Alzheimer's Disease, 72*(4), 1323–1339.

Anastasiades, P. G., & Carter, A. G. (2021). Circuit organization of the rodent medial prefrontal cortex. *Trends in Neurosciences, 44*(7), 550–563.

Andrews-Zwilling, Y., Bien-Ly, N., Xu, Q., Li, G., Bernardo, A., Yoon, S. Y., et al. (2010). Apolipoprotein E4 causes age- and tau-dependent impairment of GABAergic interneurons, leading to learning and memory deficits in mice. *Journal of Neuroscience, 30*(41), 13707–13717.

Arai, H., Emson, P. C., Mountjoy, C. Q., Carassco, L. H., & Heizmann, C. W. (1987). Loss of parvalbumin-immunoreactive neurones from cortex in Alzheimer-type dementia. *Brain Research, 418*(1), 164–169.

Arendt, T. (2009). Synaptic degeneration in Alzheimer's disease. *Acta Neuropathologica, 118*(1), 167–179.

Bachmanov, A. A., Tordoff, M. G., & Beauchamp, G. K. (1996). Ethanol consumption and taste preferences in C57BL/6ByJ and 129/J mice. *Alcoholism: Clinical and Experimental Research, 20*(2), 201–206.

Ballard, C., Mobley, W., Hardy, J., Williams, G., & Corbett, A. (2016). Dementia in Down's syndrome. *The Lancet Neurology, 15*(6), 622–636.

Barnett, A., David, E., Rohlman, A., Nikolova, V. D., Moy, S. S., Vetreno, R. P., et al. (2022). Adolescent binge alcohol enhances early Alzheimer's disease pathology in adulthood through proinflammatory neuroimmune activation. *Frontiers in Pharmacology, 13*, Article 884170.

Barthet, G., & Mulle, C. (2020). Presynaptic failure in Alzheimer's disease. *Progress in Neurobiology, 194*, Article 101801.

Batista-Brito, R., & Fishell, G. (2009). The developmental integration of cortical interneurons into a functional network. *Current Topics in Developmental Biology, 87*, 81–118.

Benz, J., Rasmussen, C., & Andrew, G. (2009). Diagnosing fetal alcohol spectrum disorder: History, challenges and future directions. *Paediatrics and Child Health, 14*(4), 231–237.

Billings, L. M., Oddo, S., Green, K. N., McGaugh, J. L., & LaFerla, F. M. (2005). Intraneuronal abeta causes the onset of early Alzheimer's disease-related cognitive deficits in transgenic mice. *Neuron, 45*(5), 675–688.

Bird, C. W., Taylor, D. H., Pinkowski, N. J., Chavez, G. J., & Valenzuela, C. F. (2018). Long-term reductions in the population of GABAergic interneurons in the mouse hippocampus following developmental ethanol exposure. *Neuroscience, 383*, 60–73.

Brady, D. R., & Mufson, E. J. (1997). Parvalbumin-immunoreactive neurons in the hippocampal formation of Alzheimer's diseased brain. *Neuroscience, 80*(4), 1113–1125.

Campsall, K. D., Mazerolle, C. J., De Repentingy, Y., Kothary, R., & Wallace, V. A. (2002). Characterization of transgene expression and Cre recombinase activity in a panel of Thy-1 promoter-Cre transgenic mice. *Developmental Dynamics, 224*(2), 135–143.

Caroni, P. (1997). Overexpression of growth-associated proteins in the neurons of adult transgenic mice. *Journal of Neuroscience Methods, 71*(1), 3–9.

Catlin, M. C., Guizzetti, M., & Costa, L. G. (1999). Effects of ethanol on calcium homeostasis in the nervous system. *Molecular Neurobiology, 19*(1), 1–24.

Chen, M., Chen, Y., Huo, Q., Wang, L., Tan, S., Misrani, A., et al. (2021). Enhancing GABAergic signaling ameliorates aberrant gamma oscillations of olfactory bulb in AD mouse models. *Molecular Neurodegeneration, 16*(1), 1–23.

Cheng, A., Wang, J., Ghena, N., Zhao, Q., Perone, I., King, M. T., et al. (2019). SIRT3 haploinsufficiency aggravates loss of GABAergic interneurons and neuronal network hyperexcitability in an Alzheimer's disease model. *Journal of Neuroscience, 40*(3), 694–709.

Chen, Y., Ozturk, N. C., Ni, L., Goodlett, C., & Zhou, F. C. (2011). Strain differences in developmental vulnerability to alcohol exposure via embryo culture in mice. *Alcoholism: Clinical and Experimental Research, 35*(7), 1293–1304.

Chui, D.-H., Tanahashi, H., Ozawa, K., Ikeda, S., Checler, F., Ueda, O., et al. (1999). Transgenic mice with Alzheimer presenilin 1 mutations show accelerated neurodegeneration without amyloid plaque formation. *Nature Medicine, 5*(5), 560–564.

Clancy, B., Darlington, R. B., & Finlay, B. L. (2001). Translating developmental time across mammalian species. *Neuroscience, 105*(1), 7–17.

Clinton, L. K., Billings, L. M., Green, K. N., Caccamo, A., Ngo, J., Oddo, S., et al. (2007). Age-dependent sexual dimorphism in cognition and stress response in the 3xTg-AD mice. *Neurobiology of Disease, 28*(1), 76–82.

Cuzon, V. C., Yeh, P. W. L., Yanagawa, Y., Obata, K., & Yeh, H. H. (2008). Ethanol consumption during early pregnancy alters the disposition of tangentially migrating GABAergic interneurons in the fetal cortex. *Journal of Neuroscience, 28*(8), 1854–1864.

Davis, K. M., Gagnier, K. R., Moore, T. E., & Todorow, M. (2013). Cognitive aspects of fetal alcohol spectrum disorder. *Wiley Interdisciplinary Reviews Cognitive Science, 4*(1), 81–92.

DeKosky, S. T., & Scheff, S. W. (1990). Synapse loss in frontal cortex biopsies in Alzheimer's disease: Correlation with cognitive severity. *Annals of Neurology, 27*(5), 457–464.

Delatour, L. C., & Yeh, H. H. (2017). FASD and brain development: Perspectives on where we are and where we need to go. *OBM Neurobiology, 1*.

Delatour, L. C., Yeh, P. W., & Yeh, H. H. (2019a). Ethanol exposure in utero disrupts radial migration and pyramidal cell development in the somatosensory cortex. *Cerebral Cortex, 29*(5), 2125–2139.

Delatour, L. C., Yeh, P. W. L., & Yeh, H. H. (2019b). Prenatal exposure to ethanol alters synaptic activity in layer V/VI pyramidal neurons of the somatosensory cortex. *Cerebral Cortex, 30*(3), 1735–1751.

Denny, C. H. (2019). Consumption of alcohol beverages and binge drinking among pregnant women aged 18–44 years – United States, 2015–2017. *MMWR Morbidity and Mortality Weekly Report, 68*(16), 365–368.

Downing, C., Balderrama-Durbin, C., Broncucia, H., Gilliam, D., & Johnson, T. E. (2009). Ethanol teratogenesis in five inbred strains of mice. *Alcoholism: Clinical and Experimental Research, 33*(7), 1238–1245.

Edwards, G. A., III, Gamez, N., Escobedo, G., Jr., Calderon, O., & Moreno-Gonzalez, I. (2019). Modifiable risk factors for Alzheimer's disease. *Frontiers in Aging Neuroscience, 11*.

España, J., Giménez-Llort, L., Valero, J., Miñano, A., Rábano, A., Rodriguez-Alvarez, J., et al. (2010). Intraneuronal beta-amyloid accumulation in the amygdala enhances fear and anxiety in Alzheimer's disease transgenic mice. *Biological Psychiatry, 67*(6), 513–521.

Fowler, S. W., Walker, J. M., Klakotskaia, D., Will, M. J., Serfozo, P., Simonyi, A., et al. (2013). Effects of a metabotropic glutamate receptor 5 positive allosteric modulator, CDPPB, on spatial learning task performance in rodents. *Neurobiology of Learning and Memory, 99*, 25–31.

Gouras, G. K., Tampellini, D., Takahashi, R. H., & Capetillo-Zarate, E. (2010). Intraneuronal beta-amyloid accumulation and synapse pathology in Alzheimer's disease. *Acta Neuropathologica, 119*(5), 523–541.

Hansen, K. B., Yuan, H., & Traynelis, S. F. (2007). Structural aspects of AMPA receptor activation, desensitization and deactivation. *Current Opinion in Neurobiology, 17*(3), 281–288.

Hardy, J., & Selkoe, D. J. (2002). The amyloid hypothesis of Alzheimer's disease: Progress and problems on the road to therapeutics. *Science, 297*(5580), 353–356.

Head, E., Lott, I. T., Hof, P. R., Bouras, C., Su, J. H., Kim, R., et al. (2003). Parallel compensatory and pathological events associated with tau pathology in middle aged individuals with Down syndrome. *Journal of Neuropathology and Experimental Neurology, 62*(9), 917–926.

Heymann, D., Stern, Y., Cosentino, S., Tatarina-Nulman, O., Dorrejo, J. N., & Gu, Y. (2016). The association between alcohol use and the progression of Alzheimer's disease. *Current Alzheimer Research, 13*(12), 1356–1362.
Hijazi, S., Heistek, T. S., Scheltens, P., Neumann, U., Shimshek, D. R., Mansvelder, H. D., et al. (2019). Early restoration of parvalbumin interneuron activity prevents memory loss and network hyperexcitability in a mouse model of Alzheimer's disease. *Molecular Psychiatry, 25*(12), 3380–3398.
Hoffman, J. L., Faccidomo, S., Kim, M., Taylor, S. M., Agoglia, A. E., May, A. M., et al. (2019). Alcohol drinking exacerbates neural and behavioral pathology in the 3xTg-AD mouse model of Alzheimer's disease. *International Review of Neurobiology, 148*, 169–230.
Huang, W.-J., Zhang, X., & Chen, & W.-W. (2016). Association between alcohol and Alzheimer's disease. *Experimental and Therapeutic Medicine, 12*(3), 1247–1250.
Iacobucci, G. J., & Popescu, G. K. (2018). Kinetic models for activation and modulation of NMDA receptor subtypes. *Current Opinion in Physiology, 2*, 114–122.
Iulita, M. F., Allard, S., Richter, L., Munter, L.-M., Ducatenzeiler, A., Weise, C., et al. (2014). Intracellular Aβ pathology and early cognitive impairments in a transgenic rat overexpressing human amyloid precursor protein: A multidimensional study. *Acta Neuropathologica Communications, 2*, 61.
Jacobson, J. L., Akkaya-Hocagil, T., Ryan, L. M., Dodge, N. C., Richardson, G. A., Olson, H. C., et al. (2021). Effects of prenatal alcohol exposure on cognitive and behavioral development: Findings from a hierarchical meta-analysis of data from six prospective longitudinal U.S. cohorts. *Alcoholism: Clinical and Experimental Research, 45*(10), 2040–2058.
Jafari, Z., Okuma, M., Karem, H., Mehla, J., Kolb, B. E., & Mohajerani, M. H. (2019). Prenatal noise stress aggravates cognitive decline and the onset and progression of beta amyloid pathology in a mouse model of Alzheimer's disease. *Neurobiology of Aging, 77*, 66–86.
Jones, K. L., & Smith, D. W. (1973). Recognition of the fetal alcohol syndrome in early infancy. *Lancet, 302*, 999–1001.
Kiss, E., Gorgas, K., Schlicksupp, A., Groß, D., Kins, S., Kirsch, J., et al. (2016). Biphasic alteration of the inhibitory synapse scaffold protein gephyrin in early and late stages of an Alzheimer disease model. *American Journal of Pathology, 186*(9), 2279–2291.
Knopman, D. S., Amieva, H., Petersen, R. C., Chételat, G., Holtzman, D. M., Hyman, B. T., et al. (2021). Alzheimer disease. *Nature Reviews Disease Primers, 7*(1), 33.
Koch, M., Costanzo, S., Fitzpatrick, A. L., Lopez, O. L., DeKosky, S., Kuller, L. H., et al. (2020). Alcohol consumption, brain amyloid-β deposition, and brain structural integrity among older adults free of dementia. *Journal of Alzheimer's Disease, 74*(2), 509–519.
Koike, M., Tsukada, S., Tsuzuki, K., Kijima, H., & Ozawa, S. (2000). Regulation of kinetic properties of GluR2 AMPA receptor channels by alternative splicing. *Journal of Neuroscience, 20*(6), 2166–2174.
Koopmans, G., Blokland, A., van Nieuwenhuijzen, P., & Prickaerts, J. (2003). Assessment of spatial learning abilities of mice in a new circular maze. *Physiology & Behavior, 79*(4–5), 683–693.
Kurucu, H., Colom-Cadena, M., Davies, C., Wilkins, L., King, D., Rose, J., et al. (2021). Inhibitory synapse loss and accumulation of amyloid beta in inhibitory presynaptic terminals in Alzheimer's disease. *European Journal of Neurology, 29*(5), 1311–1323.
Lee, S. M., Yeh, P. W. L., & Yeh, H. H. (2022). L-type calcium channels contribute to ethanol-induced aberrant tangential migration of primordial cortical GABAergic interneurons in the embryonic medial prefrontal cortex. *eNeuro, 9*(1). ENEURO.0359-21.2021.
Leon, W. C., Canneva, F., Partridge, V., Allard, S., Ferretti, M. T., DeWilde, A., et al. (2010). A novel transgenic rat model with a full Alzheimer's-like amyloid pathology displays pre-plaque intracellular amyloid-β-associated cognitive impairment. *Journal of Alzheimer's Disease, 20*(1), 113–126.
Leslie, S. W., Brown, L. M., Dildy, J. E., & Sims, J. S. (1990). Ethanol and neuronal calcium channels. *Alcohol, 7*(3), 233–236.
Leung, L., Andrews-Zwilling, Y., Yoon, S. Y., Jain, S., Ring, K., Dai, J., et al. (2012). Apolipoprotein E4 causes age- and sex-dependent impairments of hilar GABAergic interneurons and learning and memory deficits in mice. *PLoS One, 7*(12), Article e53569.
Lim, J. P., Zou, M. E., Janak, P. H., & Messing, R. O. (2012). Responses to ethanol in C57BL/6 versus C57BL/6 × 129 hybrid mice. *Brain and Behavior, 2*(1), 22–31.
Li, Y., Sun, H., Chen, Z., Xu, H., Bu, G., & Zheng, H. (2016). Implications of GABAergic neurotransmission in Alzheimer's disease. *Frontiers in Aging Neuroscience, 8*(31).
Li, Y., Zhu, K., Li, N., Wang, X., Xiao, X., Li, L., et al. (2021). Reversible GABAergic dysfunction involved in hippocampal hyperactivity predicts early-stage Alzheimer disease in a mouse model. *Alzheimer's Research & Therapy, 13*(1), 114.
Lovinger, D. M. (2018). Presynaptic ethanol actions: Potential roles in ethanol seeking. *Handbook of Experimental Pharmacology, 248*, 29–54.
Lunde, E. R., Washburn, S. E., Golding, M. C., Bake, S., Miranda, R. C., & Ramadoss, J. (2016). Alcohol-induced developmental origins of adult-onset diseases. *Alcoholism: Clinical and Experimental Research, 40*(7), 1403–1414.
Madden, J. T., Thompson, S. M., Magcalas, C. M., Wagner, J. L., Hamilton, D. A., Savage, D. D., et al. (2020). Moderate prenatal alcohol exposure reduces parvalbumin expressing GABAergic interneurons in the dorsal hippocampus of adult male and female rat offspring. *Neuroscience Letters, 718*, Article 134700.
Marguet, F., Friocourt, G., Brosolo, M., Sauvestre, F., Marcorelles, P., Lesueur, C., et al. (2020). Prenatal alcohol exposure is a leading cause of interneuronopathy in humans. *Acta Neuropathologica Communications, 8*(1), 208.
Martinez-Losa, M., Tracy, T. E., Ma, K., Verret, L., Clemente-Perez, A., Khan, A. S., et al. (2018). Nav1.1-Overexpressing interneuron transplants restore brain rhythms and cognition in a mouse model of Alzheimer's disease. *Neuron, 98*(1), 75–89.e5.
Mastrangelo, M. A., & Bowers, W. J. (2008). Detailed immunohistochemical characterization of temporal and spatial progression of Alzheimer's disease-related pathologies in male triple-transgenic mice. *BMC Neuroscience, 9*, 81.
Mattson, S. N., Crocker, N., & Nguyen, T. T. (2011). Fetal alcohol spectrum disorders: Neuropsychological and behavioral features. *Neuropsychology Review, 21*(2), 81–101.
May, P. A., & Gossage, J. P. (2011). Maternal risk factors for fetal alcohol spectrum disorders: Not as simple as it might seem. *Alcohol Research & Health, 34*(1), 15–26.
Milstein, A. D., & Nicoll, R. A. (2008). Regulation of AMPA receptor gating and pharmacology by TARP auxiliary subunits. *Trends in Pharmacological Sciences, 29*(7), 333–339.
Mitew, S., Kirkcaldie, M. T. K., Dickson, T. C., & Vickers, J. C. (2013). Altered synapses and gliotransmission in Alzheimer's disease and AD model mice. *Neurobiology of Aging, 34*(10), 2341–2351.
Moore, E. M., & Riley, E. P. (2015). What happens when children with fetal alcohol spectrum disorders become adults? *Current Developmental Disorders Reports, 2*(3), 219–227.
Möykkynen, T., & Korpi, E. R. (2012). Acute effects of ethanol on glutamate receptors. *Basic and Clinical Pharmacology and Toxicology, 111*(1), 4–13.
Muñoz, G., Urrutia, J. C., Burgos, C. F., Silva, V., Aguilar, F., Sama, M., et al. (2015). Low concentrations of ethanol protect against synaptotoxicity induced by Aβ in hippocampal neurons. *Neurobiology of Aging, 36*(2), 845–856.
Murray, A. J., Sauer, J.-F., Riedel, G., McClure, C., Ansel, L., Cheyne, L., et al. (2011). Parvalbumin-positive CA1 interneurons are required for spatial working but not for reference memory. *Nature Neuroscience, 14*(3), 297–299.
Nahar, L., Delacroix, B. M., & Nam, H. W. (2021). The role of parvalbumin interneurons in neurotransmitter balance and neurological disease. *Frontiers in Psychiatry, 12*, Article 679960.
Naseri, N. N., Wang, H., Guo, J., Sharma, M., & Luo, W. (2019). The complexity of tau in Alzheimer's disease. *Neuroscience Letters, 705*, 183–194.
Oddo, S., Caccamo, A., Shepherd, J. D., Murphy, M. P., Golde, T. E., Kayed, R., et al. (2003). Triple-transgenic model of Alzheimer's disease with plaques and tangles: Intracellular Abeta and synaptic dysfunction. *Neuron, 39*(3), 409–421.
Ogawa, T., Kuwagata, M., Ruiz, J., & Zhou, F. C. (2005). Differential teratogenic effect of alcohol on embryonic development between C57BL/6 and DBA/2 mice: A new view. *Alcoholism: Clinical and Experimental Research, 29*(5), 855–863.
Oh, K.-J., Perez, S. E., Lagalwar, S., Vana, L., Binder, L., & Mufson, E. J. (2010). Staging of Alzheimer's pathology in triple transgenic mice: A light and electron microscopic analysis. *International Journal of Alzheimer's Disease, 2010*, Article 780102.
Palop, J. J., & Mucke, L. (2016). Network abnormalities and interneuron dysfunction in Alzheimer disease. *Nature Reviews Neuroscience, 17*(12), 777–792.
Patterson, C. (2018). *World Alzheimer report 2018. The state of the art of dementia research: New frontiers*. Alzheimer's Disease International. Retrieved from https://apo.org.au/sites/default/files/resource-files/2018-09/apo-nid260056.pdf.
Peng, B., Yang, Q., Joshi, R. B., Liu, Y., Akbar, M., Song, B.-J., et al. (2020). Role of alcohol drinking in Alzheimer's disease, Parkinson's disease, and amyotrophic lateral sclerosis. *International Journal of Molecular Sciences, 21*(7), 2316.
Pietropaolo, S., Feldon, J., & Yee, B. K. (2008). Age-dependent phenotypic characteristics of a triple transgenic mouse model of Alzheimer disease. *Behavioral Neuroscience, 122*(4), 733–747.
Pimenova, A. A., Raj, T., & Goate, A. M. (2018). Untangling genetic risk for Alzheimer's disease. *Biological Psychiatry, 83*(4), 300–310.
Prince, S. M., Paulson, A. L., Jeong, N., Zhang, L., Amigues, S., & Singer, A. C. (2021). Alzheimer's pathology causes impaired inhibitory connections and reactivation of spatial codes during spatial navigation. *Cell Reports, 35*(3), Article 109008.
Ramirez, D. M., & Kavalali, E. T. (2011). Differential regulation of spontaneous and evoked neurotransmitter release at central synapses. *Current Opinion in Neurobiology, 21*(2), 275–282.
Rasmussen, C. (2005). Executive functioning and working memory in fetal alcohol spectrum disorder. *Alcoholism: Clinical and Experimental Research, 29*(8), 1359–1367.
Rasmussen, J., & Langerman, H. (2019). Alzheimer's disease – Why we need early diagnosis. *Degenerative Neurological and Neuromuscular Disease, 9*, 123–130.
Roberto, M., Treistman, S. N., Pietrzykowski, A. Z., Weiner, J., Galindo, R., Mameli, M., et al. (2006). Actions of acute and chronic ethanol on presynaptic terminals. *Alcoholism: Clinical and Experimental Research, 30*(2), 222–232.
Roberto, M., & Varodayan, F. (2017). Synaptic targets: Chronic alcohol actions. *Neuropharmacology, 122*, 85–99.
Sanchez-Mejias, E., Nuñez-Diaz, C., Sanchez-Varo, R., Gomez-Arboledas, A., Garcia-Leon, J. A., Fernandez-Valenzuela, J. J., et al. (2020). Distinct disease-sensitive GABAergic neurons in the perirhinal cortex of Alzheimer's mice and patients. *Brain Pathology, 30*(2), 345–363.
Scheff, S. W., Price, D. A., Schmitt, F. A., & Mufson, E. J. (2006). Hippocampal synaptic loss in early Alzheimer's disease and mild cognitive impairment. *Neurobiology of Aging, 27*(10), 1372–1384.
Schindelin, J., Arganda-Carreras, I., Frise, E., Kaynig, V., Longair, M., Pietzsch, T., et al. (2012). Fiji: An open-source platform for biological-image analysis. *Nature Methods, 9*(7), 676–682.

Seifan, A., Schelke, M., Obeng-Aduasare, Y., & Isaacson, R. (2015). Early life epidemiology of Alzheimer's disease – A critical review. *Neuroepidemiology, 45*(4), 237–254.
Selkoe, D. J. (2002). Alzheimer's disease is a synaptic failure. *Science, 298*(5594), 789–791.
Siggins, G. R., Roberto, M., & Nie, Z. (2005). The tipsy terminal: Presynaptic effects of ethanol. *Pharmacology & Therapeutics, 107*(1), 80–98.
Skorput, A. G. J., Gupta, V. P., Yeh, P. W. L., & Yeh, H. H. (2015). Persistent interneuronopathy in the prefrontal cortex of young adult offspring exposed to ethanol in utero. *Journal of Neuroscience, 35*(31), 10977–10988.
Skorput, A. G., Lee, S. M., Yeh, P. W., & Yeh, H. H. (2019). The NKCC1 antagonist bumetanide mitigates interneuronopathy associated with ethanol exposure in utero. *eLife, 8*, Article e48648.
Stevens, L. M., & Brown, R. E. (2015). Reference and working memory deficits in the 3xTg-AD mouse between 2 and 15-months of age: A cross-sectional study. *Behavioural Brain Research, 278*, 496–505.
Stincic, T. L., & Frerking, M. E. (2015). Different AMPA receptor subtypes mediate the distinct kinetic components of a biphasic EPSC in hippocampal interneurons. *Frontiers in Synaptic Neuroscience, 7*, 7.
Stover, K. R., Campbell, M. A., Van Winssen, C. M., & Brown, R. E. (2015). Early detection of cognitive deficits in the 3xTg-AD mouse model of Alzheimer's disease. *Behavioural Brain Research, 289*, 29–38.
Takahashi, R. H., Milner, T. A., Li, F., Nam, E. E., Edgar, M. A., Yamaguchi, H., et al. (2002). Intraneuronal Alzheimer abeta42 accumulates in multivesicular bodies and is associated with synaptic pathology. *American Journal of Pathology, 161*(5), 1869–1879.
Takahashi, K., & Yamanaka, S. (2006). Induction of pluripotent stem cells from mouse embryonic and adult fibroblast cultures by defined factors. *Cell, 126*(4), 663–676.
Tampellini, D. (2015). Synaptic activity and Alzheimer's disease: A critical update. *Frontiers in Neuroscience, 9*, 423.
Tong, B. C.-K., Wu, A. J., Li, M., & Cheung, K.-H. (2018). Calcium signaling in Alzheimer's disease & therapies. *Biochimica et Biophysica Acta Molecular Cell Research, 1865*(11 Pt B), 1745–1760.
Verret, L., Mann, E. O., Hang, G. B., Barth, A. M. I., Cobos, I., Ho, K., et al. (2012). Inhibitory interneuron deficit links altered network activity and cognitive dysfunction in Alzheimer model. *Cell, 149*(3), 708–721.
Vetreno, R. P., & Crews, F. T. (2012). Adolescent binge drinking increases expression of the danger signal receptor agonist HMGB1 and Toll-like receptors in the adult prefrontal cortex. *Neuroscience, 226*, 475–488.
Vivanti, G., Tao, S., Lyall, K., Robins, D. L., & Shea, L. L. (2021). The prevalence and incidence of early-onset dementia among adults with autism spectrum disorder. *Autism Research, 10*, 2189–2199.
Welikovitch, L. A., Do Carmo, S., Maglóczky, Z., Szocsics, P., Lőke, J., Freund, T., et al. (2018). Evidence of intraneuronal Aβ accumulation preceding tau pathology in the entorhinal cortex. *Acta Neuropathologica, 136*(6), 901–917.
Wozniak, J. R., Riley, E. P., & Charness, M. E. (2019). Clinical presentation, diagnosis, and management of fetal alcohol spectrum disorder. *The Lancet Neurology, 18*(8), 760–770.
Xu, Y., Zhao, M., Han, Y., & Zhang, H. (2020). GABAergic inhibitory interneuron deficits in Alzheimer's disease: Implications for treatment. *Frontiers in Neuroscience, 14*, 660.
Yu, J.-T., Xu, W., Tan, C.-C., Andrieu, S., Suckling, J., Evangelou, E., et al. (2020). Evidence-based prevention of Alzheimer's disease: Systematic review and meta-analysis of 243 observational prospective studies and 153 randomised controlled trials. *Journal of Neurology, Neurosurgery, and Psychiatry, 91*(11), 1201–1209.